OCEANS AND ATMOSPHERES
www.csiro.au

Review of SIOFA orange roughy (*Hoplostethus atlanticus*) acoustic data

26th FEB 2018

Feb. 2018

Scoulding, B. and Kloser, R.J. CSIRO Australia

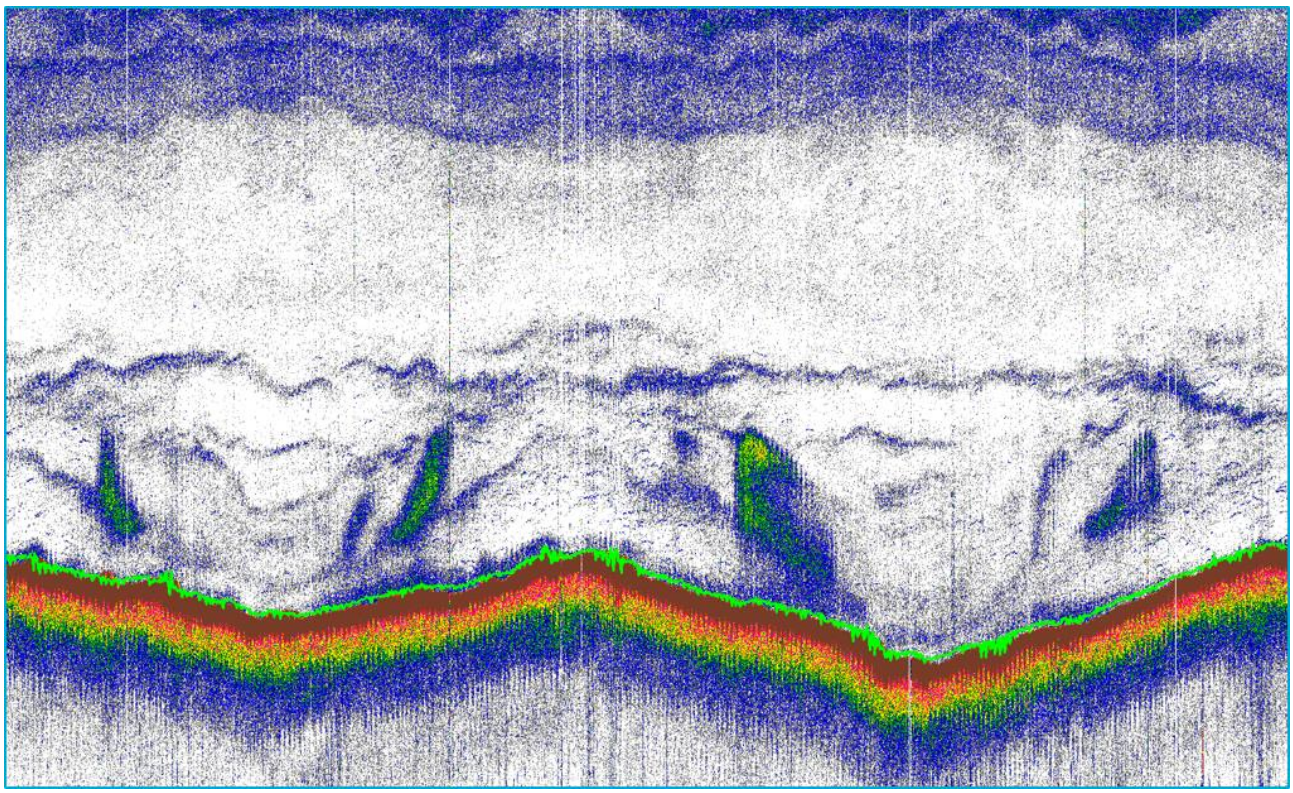

Contents

1 Introduction

This supplementary report for the South Indian Ocean Fisheries Agreement (SIOFA) details the analysis of industry acoustic data, which focuses on the third term of reference, describing in detail how the analysis was done, working through a series of calculations based on the information collected during the surveys, and the processes used to obtain numerical estimates of the abundance and other parameters of interest (Kloser *et al.*, 2018). A broad discussion of uncertainties and summary of findings with recommendations are contained within Kloser *et al.*, (2018).

1.1 Term of reference

> '*Provide an evaluation of the existing industry data, focused on one or two fishing grounds, against the adopted framework and how these data may be used within single stock assessments, as for orange roughy. This will include consideration of uncertainty in species identification, absorption, dead zone, data quality, calibration and survey strategy. This will be dependent on access to the industry data collected to date negotiated with the assistance of the SIOFA Secretariat.*'

1.2 Objectives

Biomass

1. Provide estimates of orange roughy biomass for two vessel-based acoustic surveys
2. Document the procedures used to analyse the data

Target strength and species identification

1. Provide target strength estimates for orange roughy at 38 and 120 kHz from Acoustic Optical System (AOS) measurements
2. Document the procedures used to analyse the data
3. Assess use of AOS for improving species identification

Uncertainty

1. Evaluate uncertainties associated with biomass and target strength estimates

Important parameters, symbols and units used throughout this report which are consistent with Demer *et al.*, (2015) where applicable.

Parameter	Symbol	Unit
Environmental		
Water temperature	t_w	degree Celsius (°C)
Water salinity	s_w	practical salinity unit (psu)
Water depth	d_w	metre (m)
Acoustic		
Pulse duration	τ	seconds (s)
Water sound speed	c_w	metres per second (ms^{-1})
Acoustic frequency	f	hertz (Hz) = cycles s^{-1}
Acoustic wavelength	λ	m
Acoustic wavenumber	κ	m^{-1}
Range	r	m
Absorption coefficient	α_α	dB km^{-1}
Metrics		
Signal-to-noise ratio	r_{sn}	dimensionless
Backscattering cross-section	σ_{bs}	m^2
Target strength	TS	dB re 1 m^2
Volume backscattering coefficient	s_v	m^2 m^{-3}
Volume backscattering strength	S_v	dB re 1 m^{-1}
Area scattering coefficient	s_a	m^2m^{-2}
Nautical area scattering coefficient	s_A	m^2nautical mile $(nmi)^{-2}$
Sampled volume	V_0	m^3
Inference area	a_s	nmi^2
Scatter volume density	ρ_v	number m^{-3}
Scatter abundance	n_b	number
Scatterer biomass	m_b	kilogram (kg)
Transduction		
Transmit electric power	p_{et}	watt (W)
On-axis gain	g_0 G_0	dimensionless dB re 1
Transducer beam width	θ_{-3dB}	degrees (°)
Equivalent two-way beam angle	ψ Ψ	steradian (sr) dB re 1 sr
Biological		
Standard length	SL	centimetres (cm)
Mean standard length (arithmetic $_a$ and geometric $_g$)	$\overline{SL}_a$ or $\overline{SL}_g$	cm
Weight	W	grams (g)
Mean weight (arithmetic $_a$ and geometric $_g$)	$\overline{W}_a$ or $\overline{W}_g$	g
Height of fish	H_f	cm
Width of fish	W_f	cm

Equivalent distance sampling unit	EDSU	m

1.3 Data

During the FAO/ABNJ workshop held in Rome, Italy, between 30th January and 3rd February 2017 (ABNJ Deep Seas Project, 2017), two vessel-based acoustic datasets from the Sleeping Beauty (SB) fishing ground were identified. These were made available for review and testing purposes. These are referred to as SB2005 and SB2009. In this supplementary report we document the procedures used to analyses the two datasets, accounting for a variety of potential uncertainties. The surveys were chosen as they are considered to represent good quality data with suitably low biases and errors caused by species contamination and deadzone effects. Kloser *et al.*, (2018) provides a comparison between the biomass estimates from this report and those from Niklitschek and Patchell (2015) and FAO (2017).

A third dataset from Sleeping Beauty (henceforth SB2014), containing Acoustics and Optics System (AOS) data was also identified. This dataset is evaluated for measuring target strength (*TS*, in dB re 1 m^2) of the larger (35-60 cm) orange roughy found in the southern Indian Ocean and species identification.

2 Estimating orange roughy (*Hoplostethus atlanticus*) biomass

2.1 Methods and materials

Two vessel-based acoustic datasets (SB2005 and SB2009) were collected aboard the 75 m stern trawler FV *Will Watch* (Figure 2.1). The surveys took place on the 15th and 12th July in 2005 and 2009, respectively, which coincides with the orange roughy spawning season in the Southern Indian Ocean, when fish are well aggregated and easily delineated.

2.1.1 Data

Acoustic data

The FV *Will Watch* was equipped with a hull mounted Simrad ES60 split-beam 38 kHz transducer (ES38B, serial number 30003) with a nominal 3 dB beam width (θ_{-3dB}) of 7° which gives a beam diameter of 122 m at 1000 m range. The vessels draft is 6 m and typical survey speed was between 4 and 6 ms^{-1} (8-12 knots). Acoustic data were recorded with a transmit electric power (p_{et}) of 2000 W using a pulse duration (τ) of 1.024 ms and transmit rate of ~0.5 Hz. Nominal values for sound speed in water (c_w = 1500 ms^{-1}) and absorption coefficient (α_α = 9.7472 dB km^{-1}) were used to collect the data. The settings were the same in both 2005 and 2009.

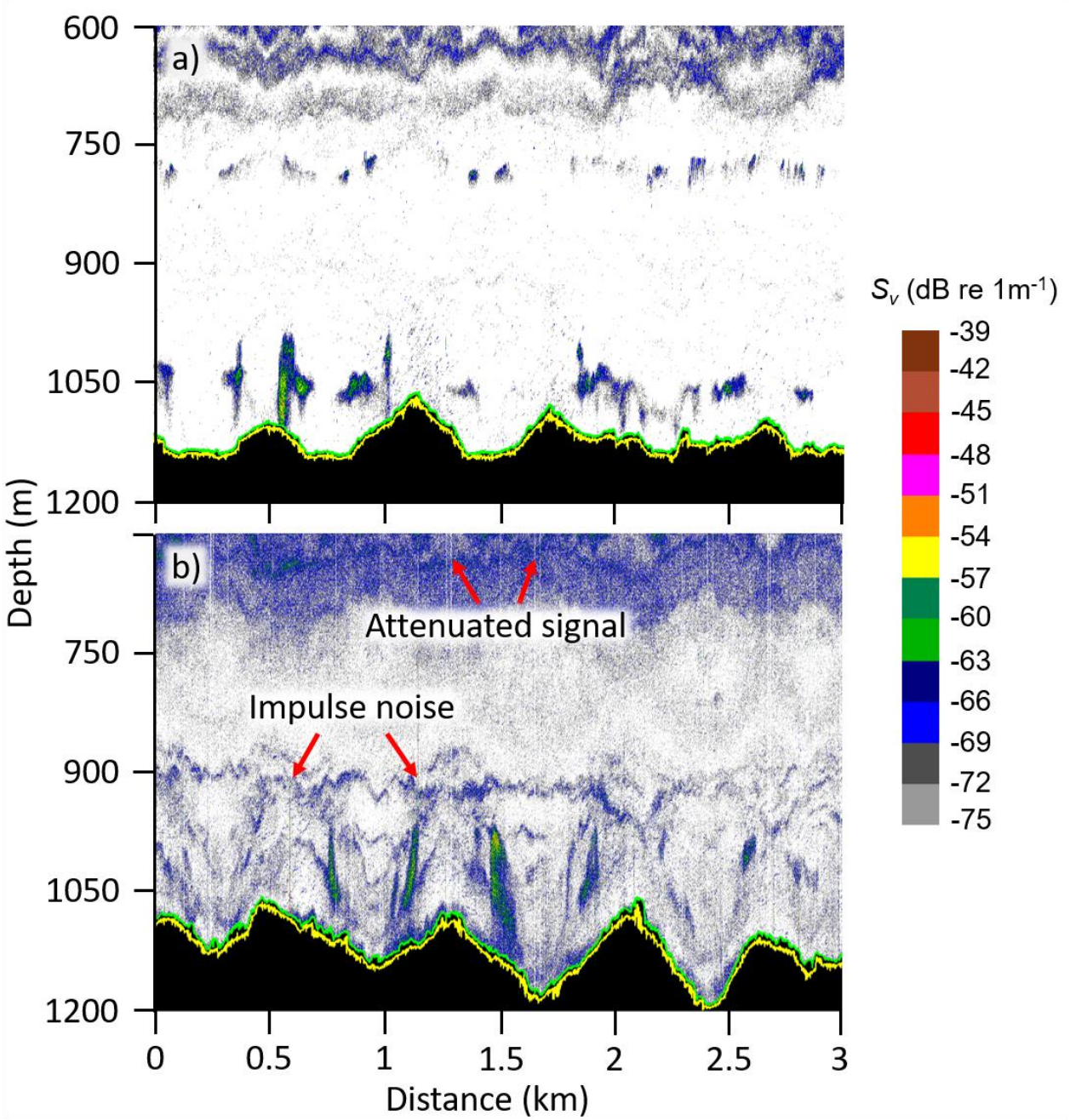

Figure 2.1 Volume backscattering strength (S_v in dB re 1 m^{-1}) echograms at 38 kHz for (a) SB2005 and (b) SB2009 acoustic surveys of orange roughy. The green line shows the acoustic detected bottom (with -2 m backstep) and the yellow line shows the true bottom (according to definitions given by Kloser (1996)).

All surveys are of a parallel transect design. The 2005 survey comprised of two smaller surveys run in sequence, the first (henceforth referred to as SB2005.1) consisted of six southwest-northeast transects (red line in Figure 2.2b) and ran between 06:55 and 07:55 UTC and the second (henceforth referred to as SB2005.2) consisted of five southeast-northwest transects (green line in Figure 2.2b) and ran between 07:57 and 08:54 UTC. The original report considered SB2005 as a single survey area but after review it is now considered as two separate surveys due to fish movement. The 2009 survey (SB2009) comprised of ten northeast-southwest transects (Figure 2.3) and ran from 05:34 to 07:14 UTC.

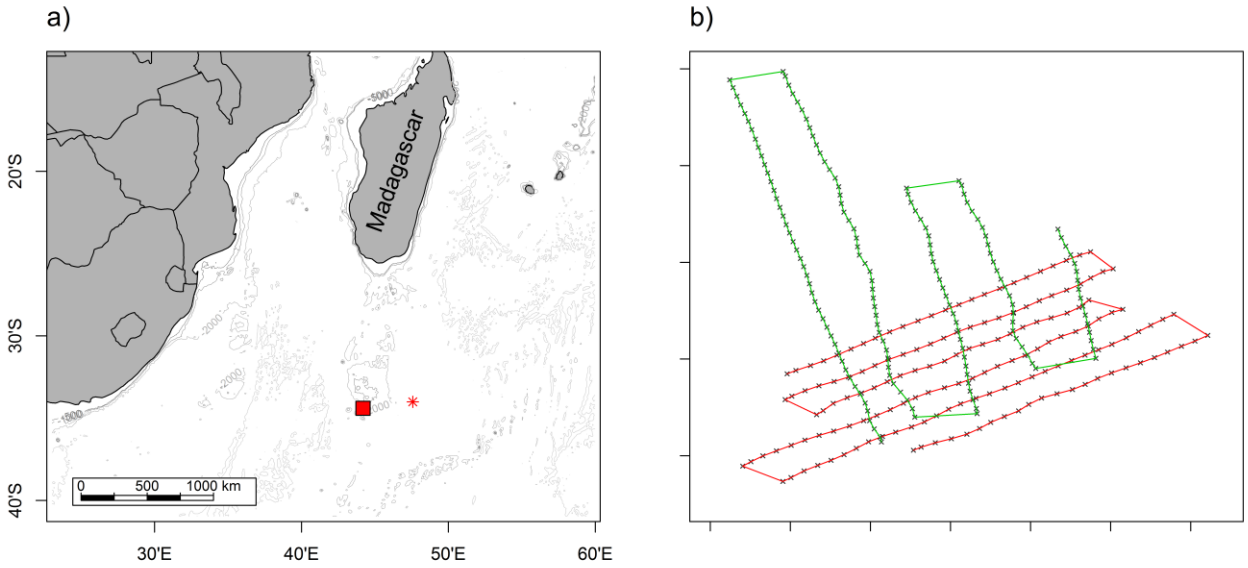

Figure 2.2 (a) Shows the approximate location (red square) of the Sleeping Beauty 2005 acoustic survey and (b) shows the cruise track of SB2005.1 (red line) and SB2005.2 (green line). Black crosses show individual 100 m intervals. The red * shows the location from where the 2005 environmental data was collected (IMOS, 2017), which is approximately 168 nautical miles away from survey area.

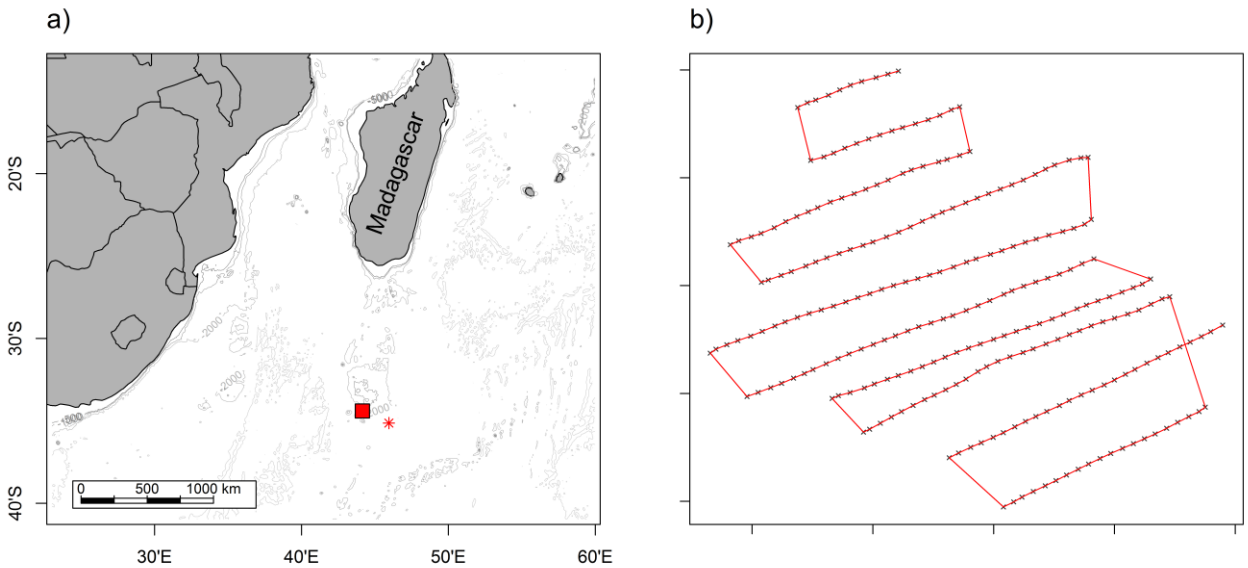

Figure 2.3 (a) Shows the approximate location (red square) of the Sleeping Beauty 2009 acoustic survey and (b) shows the cruise track (red line) of the same survey. Black crosses show individual 100 m intervals. The red * shows the location from where the 2009 environmental data was collected (IMOS, 2017), which is approximately 106 nautical miles away from survey area.

Data logging

In 2005 the data were logged using Sonardata Echolog software in the EK5 format. The data were recorded from 500 – 1400 m (sample height = 1.8 m). In 2009 data were logged in the .raw format from 500 – 1400 m using Version 1.5.2.77 of the ES60 software (sample height = 0.2 m).

Acoustic calibration

Sleeping Beauty 2005

In November 2005, the FV *Will Watch* was calibrated in Port Louis (Mauritius) following standard methods (Demer *et al*. 2015), using a 38.1 mm Tungsten Carbide (WC) sphere (theoretical *TS* = -42.4 dB re 1 m^2) by Fisheries Resource Surveys, South Africa (Soule, 2005). Echogram and echotrace data were logged using Sonardata Echolog software but raw data (.EK5) were logged directly to disc. The sea surface water temperature (t_w) was 23.5 °C and the salinity (s_w) was 35.00 psu which gave a c_w of 1531 ms^{-1} and an α_α of 9.56 dB km^{-1}. The transceiver settings at the time of the calibration are given in Table 2.1. Note no independent measurement of the beam pattern was done.

It is difficult to apply calibration settings to EK5 acoustic data files in Echoview and therefore calibration correction factors needed to be calculated. These were derived according to the following set of equations. Firstly the difference in system gain (ΔG_0, dB re 1) is given as:

$$\Delta G_0 = 2*(\text{old}G_0\text{-new}G_0), \quad (\mathbf{2.1})$$

where oldG_0 is the system gain (nominal = 26.50 dB re 1) prior to calibration and newG_0 is the new system gain derived during Echoview post processing (Eq 4.8 in Demer *et al*. 2015). The difference in area backscattering coefficient (s_a, $m^2\ m^{-2}$), s_a correction (Δs_acorr, dB re 1), is calculated as:

$$\Delta s_a\text{corr} = 2*(\text{old}s_a\text{corr-new}s_a\text{corr}), \quad (\mathbf{2.2})$$

where old$s_a$corr is the system s_a correction (nominal = 0.0, which assumes a perfectly square pulse) prior to calibration and new$s_a$corr is the new s_a correction given derived during Echoview post processing (Eq 4.9 in Demer *et al*. 2015). The overall correction (Σcorr, dB re 1) is simply:

$$\Sigma\text{corr} = \Delta G_0 + \Delta s_a\text{corr}, \quad (\mathbf{2.3})$$

which is converted to a linear correction factor ($\text{corr}_{\text{fact}}$, dimensionless) as:

$$\text{corr}_{\text{fact}} = 10\text{^}(\Sigma\text{corr}/10). \quad (\mathbf{2.4})$$

This $\text{corr}_{\text{fact}}$ is multiplied by the nautical area scattering strength (s_A, $m^2\ nmi^{-2}$) (see below) to give a corrected s_A values. The correction factor for SB2005 was 1.22 and is given in Table 2.1 along with the calibration results.

Table 2.1 ES60 transceiver settings at time of the 2005 calibration (Default) and settings once a calibration had been performed in Echoview software (Echoview). Correction factors are based on Eqs 2.1 to 2.4.

Parameter	Unit	Calibration	
		Default	Echoview
Transducer			
Frequency	Hz	38000	
Model	-	ES38B	
Serial number	-	30003	
Transceiver settings			
Serial number	-	NA	
Power	W	2000	
Pulse duration	msec	1.024	
Bandwidth	Hz	2425	
Two way beam angle	dB re 1 str	-20.6	
Angle sensitivity (both axes)	electrical°/geometric°	21.9	
Calibration settings			
Gain	dB re 1	26.50	26.45
s_a correction factor	dB re 1	0.0	-0.75
Alongship 3dB beamwidth	deg	7.10 (offset = 0.0)	*
Athwartship 3dB beamwidth	deg	7.10 (offset = 0.0)	7.17 (offset = -0.33)
Physical settings			
Absorption coefficient	dB km^{-1}	9.56	
Sound speed	ms^{-1}	1531	
Correction factor	-	-	1.22

Sleeping Beauty 2009

In May 2009, the ES60 38 kHz echosounder was calibrated off Port Louis, Mauritius, using a 38.1 mm WC (theoretical *TS* = -42.4 dB re 1 m^2) sphere suspended below the vessel following Demer *et al.*, (2015) (Soule, 2009). Sea surface t_w was 24.0 °C and s_w was assumed to be 35.0 psu, giving a c_w of 1532 ms^{-1}. The calibration was run using the ES60 software (version 1.5.2.77). The raw data files were corrected for the triangular wave error prior to post-processing (Keith *et al.* 2005). Sets of successive echoes were isolated and analysed using Echoview software (Version 4.40.71) to provide an estimate of system gain and s_a correction factor (according to Eq 4.8 and 4.9 in Demer *et al.* 2015). Calibration results are given in Table 2.2. Rather than calculating and subsequently applying a correction factor to s_A values (as for SB2005), calibration values were directly applied to the acoustic data using Echoview's .ecs calibration file. Echoview outputs are then considered to represent calibrated values.

Table 2.2 ES60 transceiver settings at time of the 2009 calibration (Default) and settings once a calibration had been performed in Echoview software.

Parameter	Unit	Calibration	
		Default	Echoview
Transducer			
Frequency	Hz	38000	
Model	-	ES38B	
Serial number	-	30003	
Transceiver settings			
Serial number	-	00907205fbb8 1	
Power	W	2000	
Pulse duration	msec	1.024	
Bandwidth	Hz	2425	
Two way beam angle	dB re 1 str	-20.6	
Angle sensitivity (both axes)	electrical°/geometric°	21.9	
Calibration settings			
Gain	dB re 1	26.50	25.45
S_A correction factor	dB re 1	0.0	-0.71
Alongship 3dB beamwidth	deg	7.10 (offset = 0.0)	6.78 (offset = -0.04)
Athwartship 3dB beamwidth	deg	7.10 (offset = 0.0)	6.85 (offset = -0.10)
Physical settings			
Absorption coefficient	dB km^{-1}	9.55	
Sound speed	ms^{-1}	1532	

Environmental data

No dedicated environmental data (e.g. conductivity, temperature and depth, CTD) were collected during either survey. It was therefore necessary to source it from elsewhere. Environmental data (temperature, salinity and depth profiles) were obtained from the Integrated Marine Observing System's (IMOS) online ocean database (https://portal.aodn.org.au/). All ARGO profiles from 2005 and 2009 data within a spatial subset were downloaded from the database. Datasets which were closest in time and space to the mean locations of the two surveys were considered acceptable.

In 2005 the closest station was approximately 168 nmi away from the location of the survey and was collected 11 days afterwards (Figure 2.2a; Table 2.3). In 2009 the station was approximately 106 nmi away and collected only two days after the survey (Figure 2.3a; Table 2.3). Given the large (1050 m) integrated depth ranges of the acoustics and the similar water masses at latitude, these stations were deemed acceptable for the purpose of this study.

A CTD cast (deployed on the Acoustic Optical System (AOS)) was done at the Sleeping Beauty fishing ground in July 2014. The results from this CTD cast were compared with the environmental data obtained from IMOS in 2005 and 2009 and were found to have very similar temperature and salinity profiles (Table 2.3, Figure 2.4).

Table 2.3 Summary of environmental datasets obtained from the IMOS database in 2005 and 2009 and the CTD deployment in 2014.

Year	Month	Day	Min depth (m)	Max depth (m)	Temperature (°C)		Salinity (psu)		Distance from survey (nmi)	Time from survey (days)
					20 m	1050 m	20 m	1050 m		
2005	07	26	16	1983	16.96	7.48	36.05	34.96	168	+ 11
2009	07	14	6	2000	17.38	6.36	35.59	34.45	106	+ 2
2014	07	05	3	1145	17.92	7.41	35.63	34.85	0	+ 1

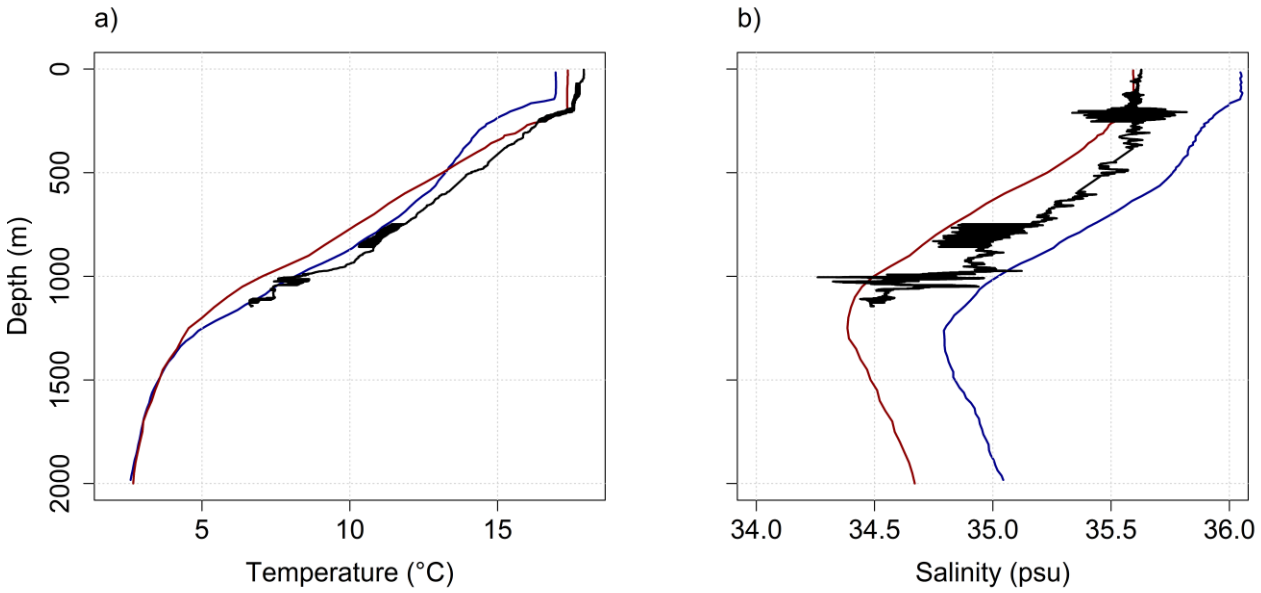

Figure 2.4 Temperature (a) and salinity (b) profiles with depth for SB2005 (blue) and SB2009 (red) acoustic surveys of orange roughy. Data were obtained from the Integrated Marine Observing System (IMOS) online database (see Table 2.3 for details). Black lines are data taken from a CTD cast taken at Sleeping Beauty in 2014.

Biological data

Biological data were collected at the survey time and were used to verify acoustic observations and determine the sex, length and weight of the individuals in the sampled population. Length is given as standard length (*SL*, measured from tip of the snout to the posterior end of the last vertebrae, in cm) and weight (*W*, is total weight in grams). Length is fed in to the target strength to length (*TS*-*SL*) equation (see below) and weight is used to scale abundance (e.g. number of individuals in the inference area) in to biomass (in tonnes). Biological data is also required to derive length-weight (*SL*-*W*) relationships by sex.

Biological data (SL, W, and sex) for Sleeping Beauty were made available for catch records from 2005-2015. Geometric mean standard lengths ($\overline{SL_g}$) (Figure 2.5) and arithmetic mean weights ($\overline{W_a}$) of male and female orange roughy from 2005-2015 are summarised in Table 2.4. Female orange roughy are consistently larger and heavier than males, with $\overline{SL_g}$ of 45.1-48.9 cm (1 standard deviation (SD) 2.9-3.1 cm) and a $\overline{W_a}$ of 3000-3768 g (SD 575-823 g), compared to males which have a $\overline{SL_g}$ of 42.9-45.7 cm (1 SD 2.5-3.2 cm) and a $\overline{W_a}$ of 2297-2739 g (SD 419-500 g). When all years are taken together, the $\overline{SL_g}$ and $\overline{W_a}$ of female orange roughy are 46.4 cm (SD 3.1 cm) and 3177 g (SD 640 g), respectively, compared to males which had a $\overline{SL_g}$ and $\overline{W_a}$ of 43.0 cm (SD 2.6 cm) and 2557 g (SD 487 g) respectively. Length distributions of male and female orange roughy sampled between 2005 and 2015 are shown in Figure 2.6. The SL_g is reported as it can go straight in to the target strength equation (see below) accounting for the length frequency distribution.

It is worth noting that the weight measurements given assume that the scales used on board the *FV* Will Watch are correct.

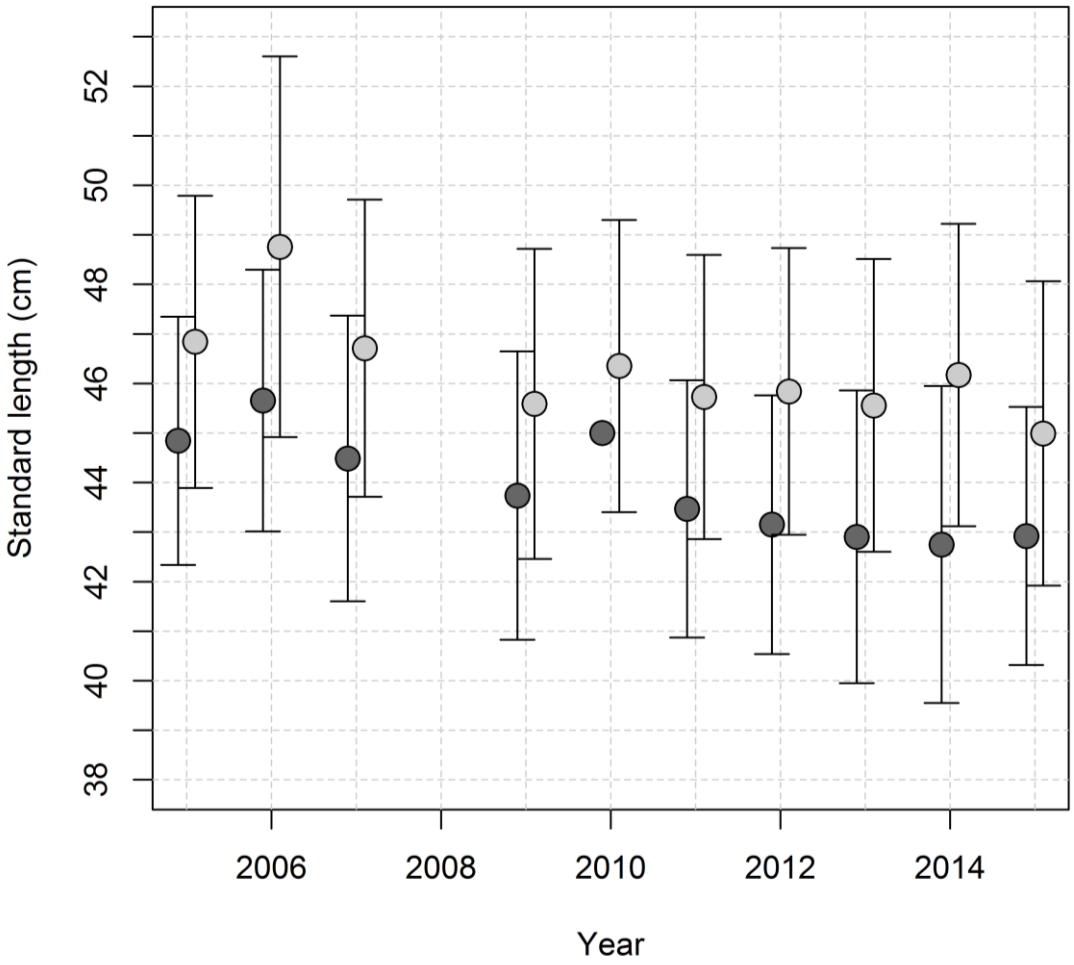

Figure 2.5 Geometric mean standard length by year for male (dark grey circles) and female (light grey circles) orange roughy. The error bars show ± 1 standard deviation of the geometric mean. The points representing male and female are slightly offset as to make the error bars distinguishable. No error bar is shown for male orange roughy in 2010 as measurements were only made on one fish. Also see Table 2.4.

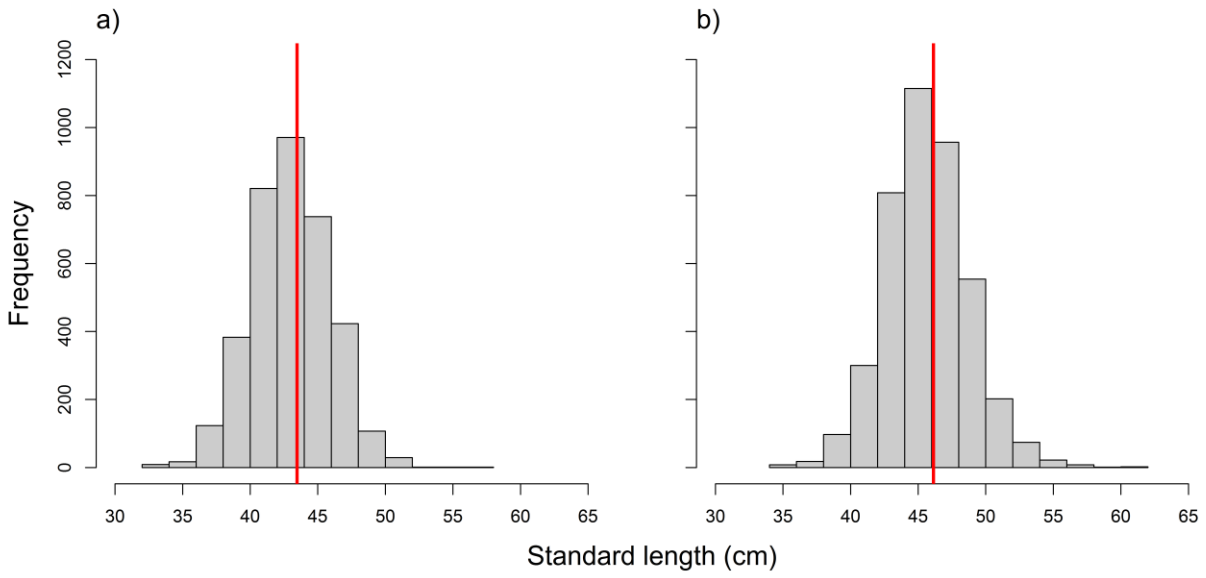

Figure 2.6 Length frequency distributions for male (a) and female (b) orange roughy for individuals sampled from commercial catch between 2005 and 2015. Vertical red lines indicate geometric mean standard length (cm). N = 3829 and 4343 for male and females respectively.

Biological values relevant to SB2005 and SB2009 are highlighted in red in Table 2.4. When equal numbers of male and female are assumed to occur (i.e. 1:1 sex ratio) the combined $\overline{SL_g}$ for 2005 and 2009 was 45.6 and 44.5 cm, respectively. Mean arithmetic weight (determined from Eqs 2.5 and 2.6) was 2979 and 2771 g, respectively. These values are used in estimations of biomass for SB2005 and SB2009. It should be noted that many more fish were sampled in 2009 (n = 1541) compared to 2005 (n = 151).

Table 2.4 Summary of biological data by year for female and male orange roughy from 2005-2015. Note that no samples were available in 2008. $\overline{SL}_g$ = geometric mean standard length (cm) and $\overline{W}_a$ = arithmetic mean weight (g). N = number of individuals measured. The mean values of all years are given in the last row. Values appropriate to SB2005 and SB2009 are highlighted in bold red lettering. SD is the standard deviation.

Year	Female					Male				
	$\overline{SL}_g$ (cm)	SD of *SL* (cm)	$\overline{W}_a$ (g)	SD of *W* (g)	N	$\overline{SL}_g$ (cm)	SD of *SL* (cm)	$\overline{W}_a$ (g)	SD of *W* (g)	N
2005	**46.8**	**2.9**	**NA**	**NA**	**58**	**44.8**	**2.5**	**NA**	**NA**	**93**
2006	48.8	3.8	3768	823	191	45.7	2.6	2739	487	109
2007	46.7	3.0	3125	584	670	44.5	2.9	2573	493	225
2008	-	-	-	-	-	-	-	-	-	-
2009	**45.6**	**3.1**	**3088**	**646**	**646**	**43.7**	**2.9**	**2658**	**500**	**895**
2010	46.4	2.9	3119	662	99	45.0	NA	2730	NA	1
2011	45.7	2.9	3175	605	859	43.5	2.6	2602	434	315
2012	45.8	2.9	3135	599	894	43.2	2.6	2518	419	905
2013	45.6	3.0	3072	614	386	42.9	3.0	2414	486	613
2014	46.2	3.1	3000	575	268	42.7	3.2	2297	480	428
2015	45.0	3.1	3107	653	155	42.9	2.6	2557	487	245
Mean	46.3	3.1	3114	640	-	43.9	2.8	2527	473	-

Here, the *SL*-*W* relationship used was determined by fitting a linear model to the log transformed weight and length measurements taken from the Sleeping Beauty fishing ground between 2005 and 2015 (Figure 2.7). Male (n = 3624) and females (n = 4166) were analysed separately to give the following equations:

$$W_m = 0.3348\ SL^{2.3636}, \quad \textbf{(2.5)}$$

and

$$W_f = 0.2267\ SL^{2.4856}, \quad \textbf{(2.6)}$$

where W_m and W_f are weight in grams for males and females respectively.

The *SL*-*W* relationships given in Eqs 2.5 and 2.6 were compared to two existing *SL*-*W* equations given by Lyle *et al.* (1991) and Kloser *et al.* (2017), which are based on a smaller size range of orange roughy (~20 to 50 cm) (see Table 2.5 for parameters and Figure 2.7 for relationship). Based on a standard length of 45 cm (approximate mean length of a Sleeping Beauty individual) the weight of male and female orange roughy were determined using each of the *SL*-*W* relationships (Table 2.5). For a 45 cm orange roughy the weight estimated using the equations given by Lyle *et al.* (1991) and Kloser *et al.* (2017) were respectively -6.6% and +3.3% compared to the current *SL*-*W* for males and -11.9% and -2.1% for females, respectively. These differences scale directly to biomass.

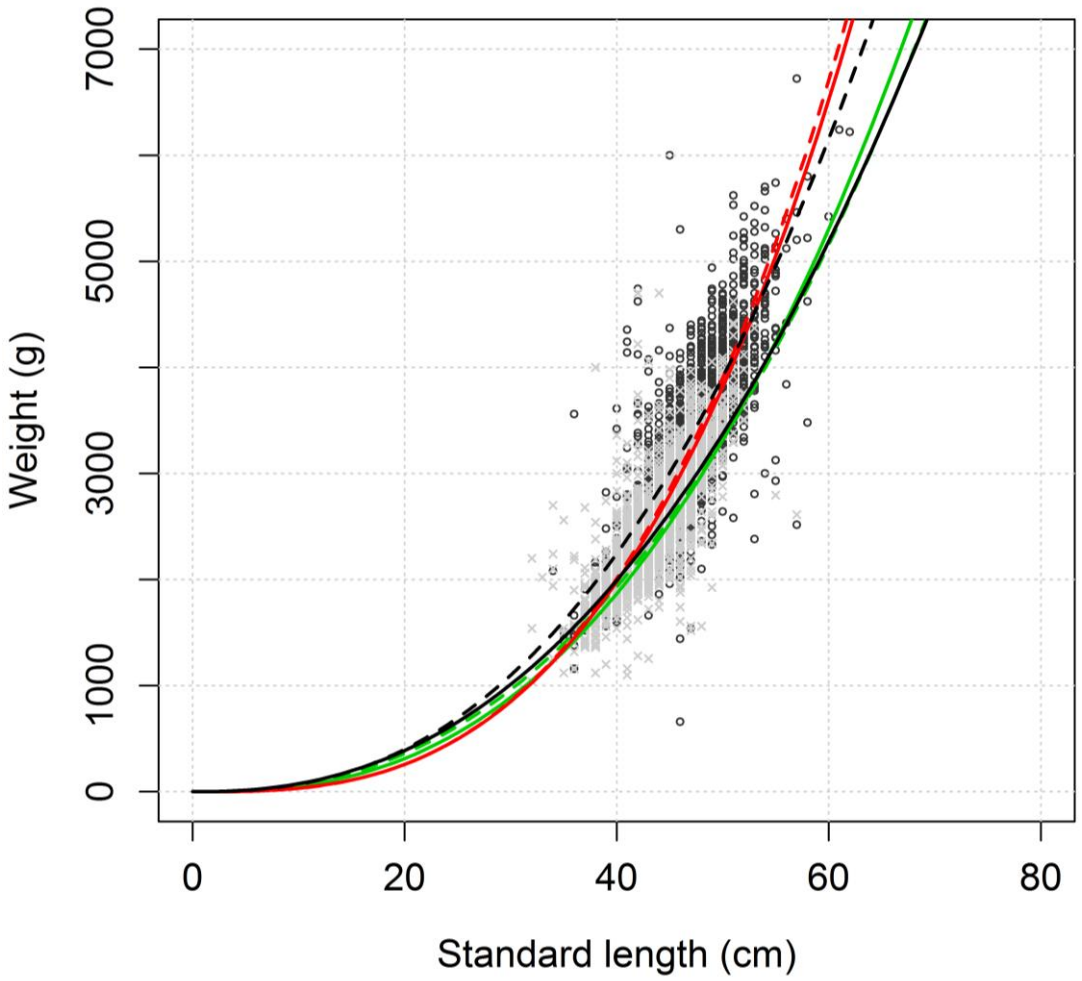

Figure 2.7 Standard length (SL, cm) vs weight (W, g) for male (light grey crosses) and female (dark grey circles) orange roughy from sleeping beauty fishing ground from 2005-2015. The length-weight relationship for this dataset is given for male weight (g) = 0.33 $SL^{2.36}$ (solid black line) and female weight (g) = 0.23 $SL^{2.49}$ (dashed black line). The length-weight relationships as determined by Lyle *et al* (1991) for male weight (g) = 0.1387 $SL^{2.5772}$ (solid green line) and female weight (g) = 0.2527 $SL^{2.4238}$ (dashed green line). The length-weight relationships as determined by Kloser *et al* (2017) for male weight (g) = 0.0383 $SL^{2.942}$ (solid red line) and female weight (g) = 0.0351 $SL^{2.97}$ (dashed red line).

Table 2.5 Standard length-weight parameters derived from the current study and taken from Lyle *et al* (1991) and Kloser *et al*. (2017). Weight is given for a 45 cm orange roughy. The difference % refers to the percentage of the weight estimate above or below that derived from using the standard length-weight relationship derived from this study.

Sex	Intercept	Slope	Weight (g)	Difference (%)	Source
Male	0.3348	2.3636	2706	-	Current
	0.1387	2.5772	2528	-6.6%	Lyle et al. (1991)
	0.0383	2.9420	2799	+3.3%	Kloser et al. (2017)
Female	0.2267	2.4856	2915	-	Current
	0.2527	2.4238	2568	-11.9%	Lyle et al. (1991)
	0.0351	2.9700	2853	-2.1%	Kloser et al. (2017)

Other data

Global Positioning System (GPS) information were logged by the vessels on board GPS system as NMEA sentence GPGGA. The vessel did not have a Motion Reference Unit (MRU) installed on board and therefore acoustic data could not be corrected for the effects of motion (i.e. pitch, roll and heave) (Dunford, 2005).

2.1.2 Data processing and interpretation

Echoview processing

Processing of the acoustic data was done using Echoview version 8.0.84 (Echoview software, 2017). The following sections describe the acoustic processing procedure carried out in Echoview, which is summarised in Figure 2.8. For SB2009 calibration values were manually changed in the ecs file. For both SB2005 and SB2009 cumulative sound speeds were entered in Echoview as part of an .ecs calibration file, these were 1510 and 1512 ms^{-1} for SB2005 and SB2009 respectively.

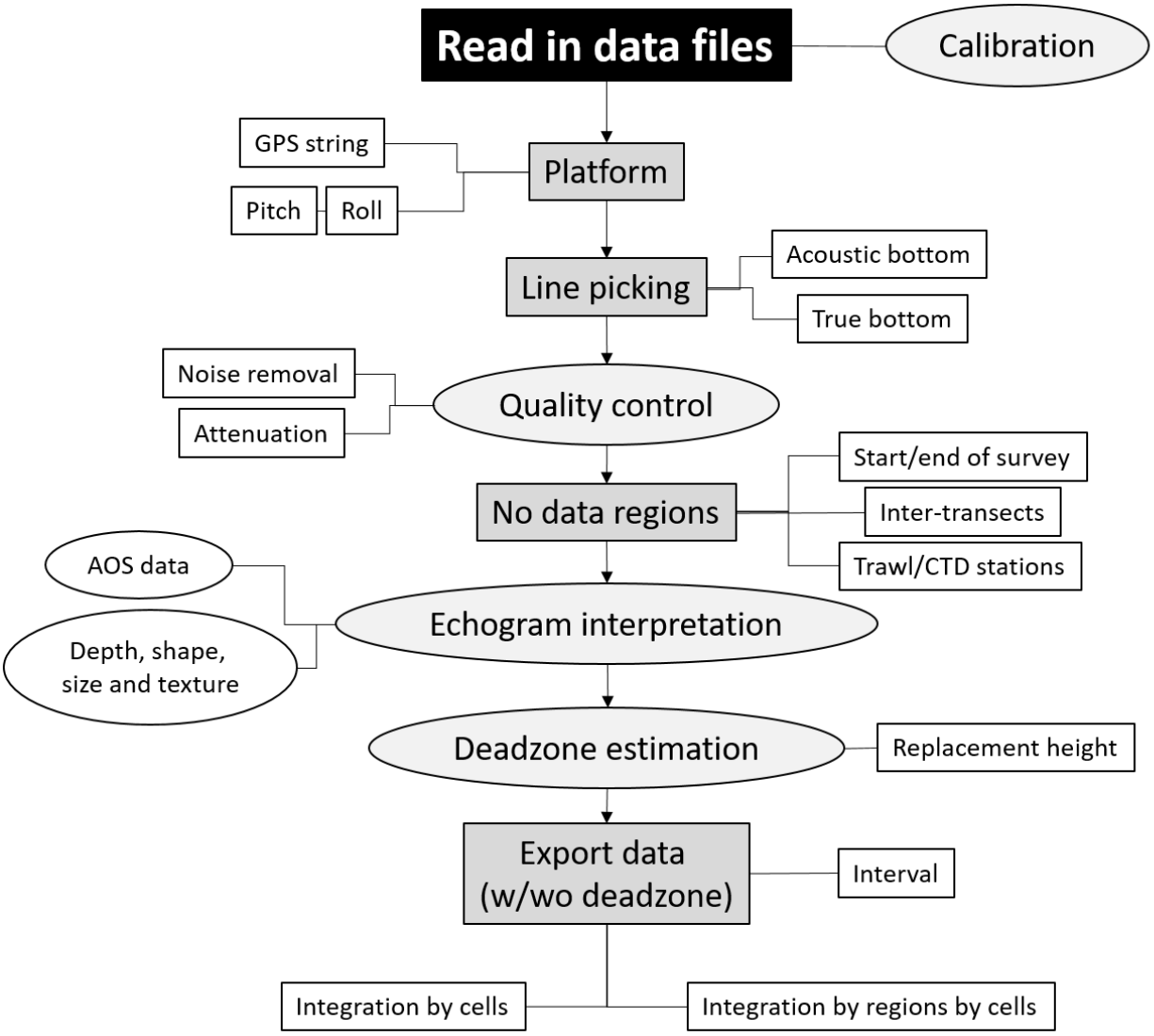

Figure 2.8 Flowchart of basic processing steps carried out in Echoview. Dark grey boxes indicate processing steps, white boxes show sub-steps or outputs, the light grey ovals indicate sources of potential error and white ovals indicate sources of axillary information.

Echogram quality control

Following visual inspection of the 38 kHz S_v echograms, the quality of the acoustic data recorded by the FV *Will Watch* during the SB2005 and SB2009 surveys was considered acceptable for analysis, with suitably high signal to noise, allowing for easy delineation of [assumed] orange roughy aggregations and the seabed. On occasion, however, the signal was attenuated (masked) by air bubbles beneath the transducer or corrupted by impulse (spike) noise (see Figure 2.1b), possibly caused by breaking waves causing reverberation within the vessels hull. Attenuated and corrupted pings respectively underestimate and overestimate acoustic density and therefore need to be removed from analysis. Typically, a semi-automatic procedure is applied to isolate attenuated or corrupted pings (collectively referred to as 'bad' data) following procedures described by Ryan *et al.* (2015). These filters are now available as single operators in Echoview. On occasion, these filters fail to identify bad pings and therefore it can be necessary to cross-validate their effectiveness and manually remove any bad pings which remain. In all cases bad pings should be removed from analysis. It is generally not considered appropriate to apply correction factors to missing data. Due to the small number of attenuated or corrupted pings within the data (0 and 5 in SB2005 and SB2009, respectively) all pings were identified and removed manually. Only bad

pings associated with assumed orange roughy aggregations were identified and removed as bad pings elsewhere do not influence echo integration and subsequent biomass estimates as these regions are masked (i.e. excluded) from analysis.

Additional sources of noise include, background noise (e.g. caused by engine/propeller noise) and biological noise (e.g. backscatter contributions from non-orange roughy, e.g. zooplankton and fish with swimbladders). It was assumed that schools contained no other species and that background noise contained no orange roughy, however both are unknown. The data quality in both years was considered acceptable with low levels of background noise (BNG) (mean = -141.69 and -146.66 dB re 1 m^{-1} for 2005 and 2009 respectively) and no interference from other acoustic systems (Figure 1.1). As a result it was deemed unnecessary to apply background noise removal algorithms (e.g. De Robertis and Higginbottom, 2007) to the data. In 2005 biological noise appeared less compared to 2009 (Figure 2.1) making delineation of school regions assumed to be 100% orange roughy easier. It is possible that in 2009 non-orange roughy targets were included in the analysis. However, without any directed biological sampling this is difficult to infer and it was considered inappropriate to apply a correction factor which corrects for apparent biological noise, particularly in the absence of dedicated biological samples. It is also likely that orange roughy were outside aggregations and we assume these factors cancel out.

Removal of bad data regions

In addition to removing bad data caused by noise it is necessary to remove bad regions outside of the inference area (i.e. start and end of the survey), inter-transects and, if present, CTD and trawl stations. This was achieved using the cruise tracking window displayed in Echoview. Non-survey regions and inter-transects were manually delineated and marked as bad data, which were then excluded from analysis.

Acoustic deadzone estimate

The acoustic deadzone (or shadow zone) is a region adjacent to the seabed where it is not possible to distinguish signal from the water column (e.g. orange roughy aggregations) with signal from the seabed (Kloser, 1996) and is caused by physical characteristics of the transmit pulse, the acoustic beam (Ona and Mitson, 1996) and by the gradient of the seabed (Kloser, 1996). This is particularly problematic for semi-demersal species, like orange roughy, which can associate closely with the seabed with steep slopes. It is therefore necessary to account for the potential biomass lost within the deadzone. Here we apply the methods described in Kloser (1996), as implemented in Echoview. The deadzone is identified using two lines, an 'acoustic bottom' line (where seabed backscatter begins to mask water column signal) and a 'true bottom' line (the highest acoustic signal for each ping (below the transmit pulse)) (Figure 2.9b). The acoustic bottom line was generated using Echoview's best bottom candidate algorithm (detection parameters are given in Table 2.6). To prevent inclusion of seabed backscatter a back-step of 2 m was applied. If necessary this line was manually altered to ensure that contamination by seabed signal was prevented. A 'true seabed' line was then defined based on the maximum S_v value for each ping (using the maximum S_v algorithm in Echoview, see Table 2.6). Each data sample in the deadzone (i.e. the area between the acoustic and true seabed lines) is replaced by the average of the S_v signal in the 5 metres (user defined) directly above the acoustic seabed line. This is based on the assumption that the density of fish directly above the acoustic bottom is on average representative of the density within the deadzone region. The virtual echogram that is created can be analysed, with the true

bottom as an exclude-below line, to produce an estimate of the proportion of fish in the deadzone.

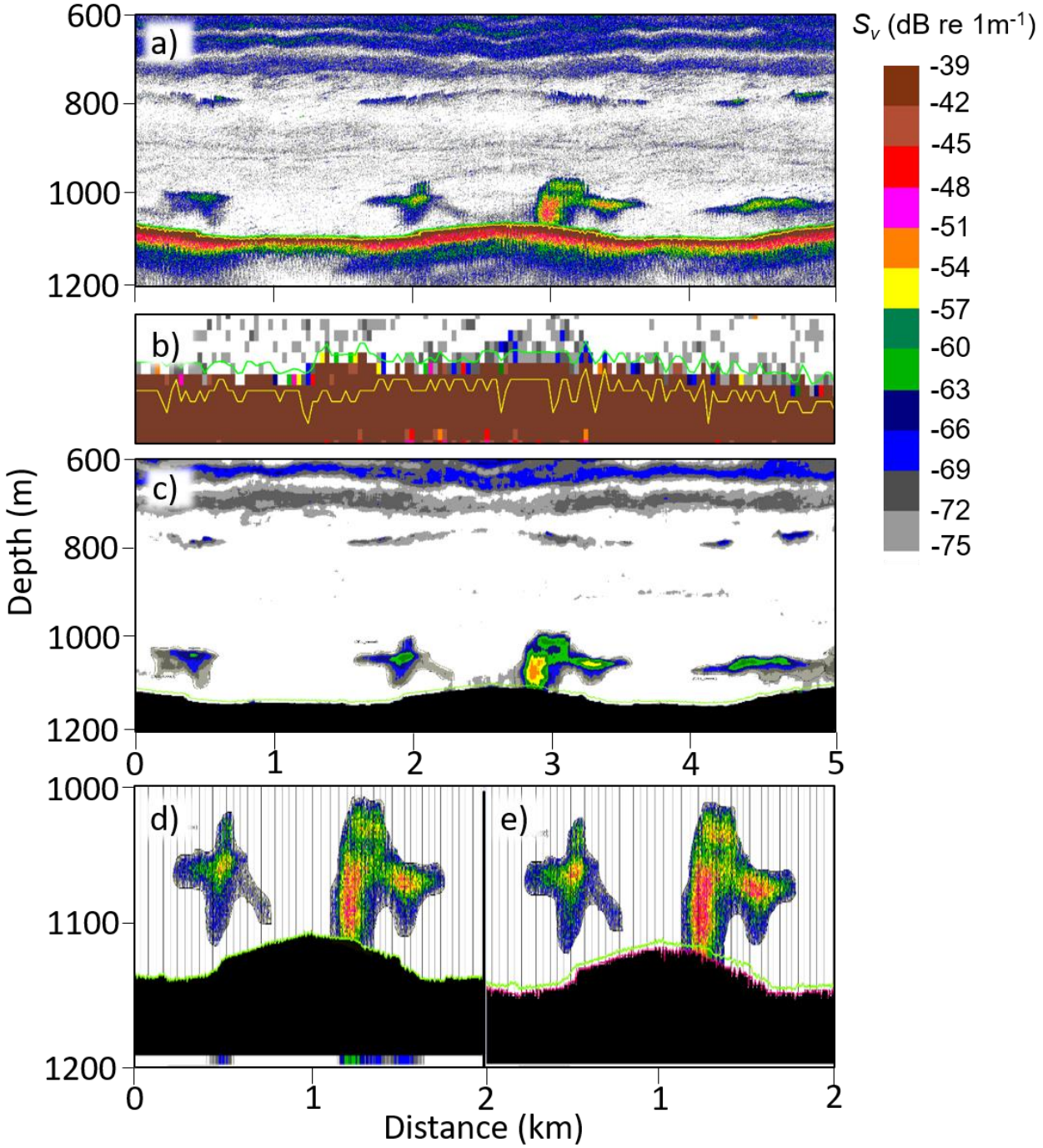

Figure 2.9 A simple representation of the echogram interpretation procedure carried out in Echoview software: (a) Sv echogram at 38 kHz, (b) section of the seafloor showing the acoustic bottom (green line) and true bottom (yellow line), (c) an XxY 7x7 25th percentile echogram used to remove weak water column scatterers and to improve delineation fish aggregations, (d) masked echogram showing regions assumed to contain 100% orange roughy (deadzone excluded) and (e) masked echogram showing regions identified as orange roughy (deadzone included). The vertical lines in d and e show the 100 m intervals used for integration analysis. The colour scale is the volume backscattering strength (S_v, in dB re 1 m^{-1}).

Table 2.6 Parameters used in the detection of the acoustic bottom and true bottom according to definitions given by Kloser (1996) as implemented in Echoview software.

Parameter	Line	
	Acoustic bottom	True bottom
Line picking algorithm		
Algorithm	Best bottom candidate	Maximum S_v
Basic settings		
Start depth (m):	600	600
Stop depth (m):	1400	1400
Minimum Sv for good pick (dB):	-70	-70
Backstep		
Use Backstep	X	X
Discrimination level (dB):	-50.00	X
Backstep range (m):	2	X
Advanced settings		
Peak threshold (dB):	-50.00	X
Maximum dropouts (samples):	2	X
Window radius (samples):	8	X
Minimum peak asymmetry:	-1.00	X

Echogram interpretation and school delineation for unsupervised data collection

Typically, echogram interpretation (commonly referred to as manual scrutiny) is guided by information given from multiple data sources. If available, multiple-frequency data (i.e. simultaneously operating more than one narrowband echosounder, e.g. 38 and 120 kHz) allows different target groups to be distinguished from one another. As objects scatter sound differently at different frequencies (e.g. swimbladdered fish scatter more sound at 38 kHz compared to non-swimbladderd fish), analysts are broadly speaking able to separate orange roughy from non-orange roughy aggregations (e.g. fish with swimbladders) (Ryan and Kloser, 2016). This does become more difficult when mixed species aggregations occur. Furthermore, interpretation is typically supported by additional evidence, e.g. catch data or video footage/camera stills. In the absence of such information, as was the case in the SB2005 and SB2009 surveys, echogram interpretation is solely reliant on expert judgement (where depth, location, shape, school dynamics, and texture are considered) and, if possible, through anecdotal consultation with the fishing industry (e.g. skipper) and referral to [historical] catch records in the area. This approach can lead to a level of subjectivity and subsequent uncertainty which ultimately tracks through to biomass estimation. Interpretation of echograms is made more difficult when fish are not properly aggregated and individuals are loosely distributed around the main aggregations. Here the display threshold (that is the display thresholds (upper and lower) of the echogram) used to identify aggregations is also important. Too low a display threshold may include loosely scattered non-orange roughy targets, whereas, too high a display threshold is likely to exclude orange roughy from analysis, leaving only strong (likely swimbladdered) targets. In this study the S_v display threshold used was between -75 and -39 dB re 1 m^{-1}. Note that this threshold is purely visual and does not affect the underlying acoustic values. The two datasets (SB2005 and 2B2009) comprised of assumed orange roughy schools which could be clearly delineated from surrounding

backscatter. To improve our ability to delineate aggregated fish from scattered individuals an XxY statistic operator was used in Echoview. This operator applies a convolution window (7 x 7 in this case) on the specified statistic (here the 25th percentile) (Figure 2.9c). Rectangular regions were then drawn around orange roughy aggregations based on interpretation of this virtual echogram. The regions were then manually altered based on the actual (i.e. non-rectangular) shape of the aggregation.

Echo-integration and export

Cruise tracks were divided into 100 m intervals (elementary distance sampling units or EDSU), which were integrated using Echoview, and exported as 'analysis by cells' and 'analysis by regions by cells'. Data were exported from two variables on which biomass estimation would be based (i) above the 'acoustic bottom' (exclusion of deadzone) and for (ii) above 'true bottom' (inclusion of deadzone).

Data processing in R

Once aggregations defined as orange roughy had been exported from Echoview the outputs were processed in the R statistical computing programme (R core team, 2017). A number of R packages were used to process the data, these include: 'raster', 'geosphere', 'pracma', 'spatstat', 'sp', 'maps', 'mapdata', 'mapproj', 'maptools', 'marmap', 'RGeostats', 'gwidgets', 'Rcpp', 'ggplot2', 'utils', 'cowplot', 'fields', 'shapefiles', 'ggmap', 'rworldmap', 'rworldextra', 'rgdal' and 'scales'.

The processing steps performed in R, are summarised in Figure 2.10 and described in detail below.

Data requirements

Three data types are required to perform post-processing in R (Figure 2.10). These are;

1) Acoustic data: direct exports from Echoview ('integration by cells' and 'integration by regions by cells').
2) Environmental data: temperature, salinity and depth profiles (here taken from the IMOS oceans database).
3) Biological data: standard length, weight and sex ratios (obtained from historical catch records from 2005-2015). Length-to-weight relationships are given in Eqs 2.5 and 2.6.

A fourth type may also be considered; data collected from a motion reference unit or a GPS.

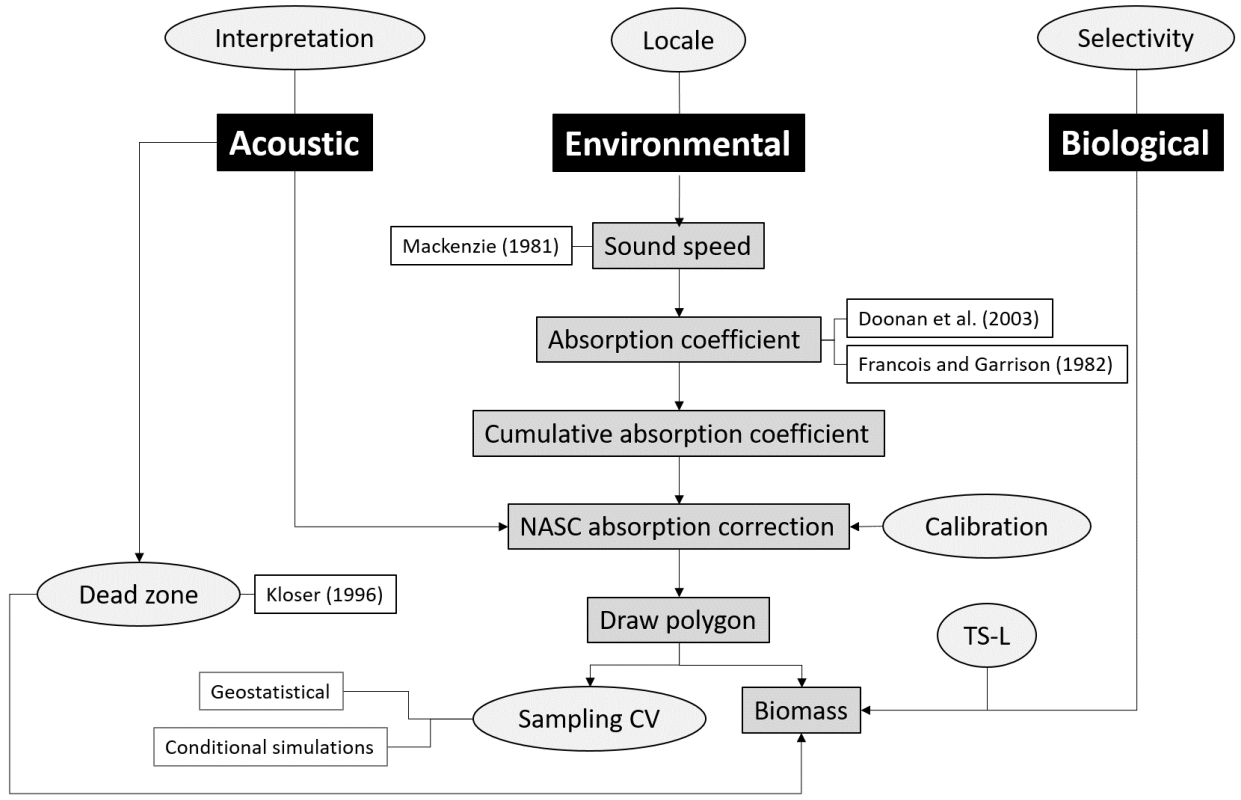

Figure 2.10 Flowchart showing processing steps in R. Black boxes represent data inputs, dark grey boxes indicate processing steps, white boxes show sub-steps or references, and the light grey ovals indicate sources of potential error.

Absorption correction factor

Prior to calculating cumulative absorption, cumulative sound speed and subsequent correction factors it is important to ensure that the environmental profiles (e.g. temperature and salinity) consist of equally spaced samples in terms of depth (e.g. depth interval of 10, 20, 30, 40…and so on). In 2005 the samples were separated in range by 25 m, and in 2009 and 2014 by 50 m.

Acoustic data were collected using nominal absorption coefficients (α_{α}nom) of 9.75 dB km^{-1} in both 2005 and 2009. Echoview applies this absorption coefficient to all acoustic samples. However, this is not the correct procedure and it was therefore necessary to determine absorption correction factors over the depth ranges being investigated. Sound speed (c_w, in ms^{-1}) was calculated using the equations given in Mackenzie (1981) based on the IMOS environmental data (Figure 2.11a). The subsequent sound speed profile was then used to estimate the absorption coefficient (α_{α}, in dB km^{-1}) along the same depth profile according to the equations of Francois and Garrison (1982) and Doonan *et al.* (2003) (Figure 2.11b). The cumulative mean absorption coefficient $\overline{\alpha_{\alpha}cum}$ was calculated as:

$$\overline{\alpha_{\alpha}cum} = \frac{\alpha_{\alpha}cum}{n_{1+i}}, \qquad \textbf{(2.7)}$$

where $\alpha_{\alpha}cum$ is the cumulative absorption coefficient and n_{1+i} is the number of observations over which $\alpha_{\alpha}cum$ is calculated. Cumulative absorption coefficients began at the transducer depth (i.e. vessel draft = 6 m).

Next the mean depth $\overline{d_z}$ (m) of each orange roughy aggregation within each export cell was determined from the two Echoview export files. The $\overline{d_z}$ is matched with the appropriate $\overline{\alpha_\alpha cum}$ at the same depth. This was done for $\overline{\alpha_\alpha cum}$ calculated using both the Francois and Garrison (1982) and Doonan *et al.* (2003) equations.

Absorption correction factors ($\alpha_\alpha$corr) for two-way propagation loss were calculating according to:

$$\alpha_\alpha\text{corr} = 10^{\frac{2\cdot(\overline{\alpha_\alpha cum}-\alpha_\alpha nom)\cdot\overline{d_z}}{10}}. \quad \textbf{(2.8)}$$

The $\alpha_\alpha$corr values were applied to the s_A values in each cell as:

$$s_A\text{corr} = s_A \cdot \alpha_\alpha\text{corr}. \quad \textbf{(2.9)}$$

A separate $\alpha_\alpha$corr is calculated for each cell as the value is dependent on the mean depth of the aggregation within the cell. All biomass estimates were based on the absorption corrected s_A values.

The cumulative absorption coefficients at 1100 m, as determined by Francois and Garrison (1982) and Doonan *et al.* (2003) and the corresponding absorption correction factors at the same depth, for 2005 and 2009, are given in Table 2.7.

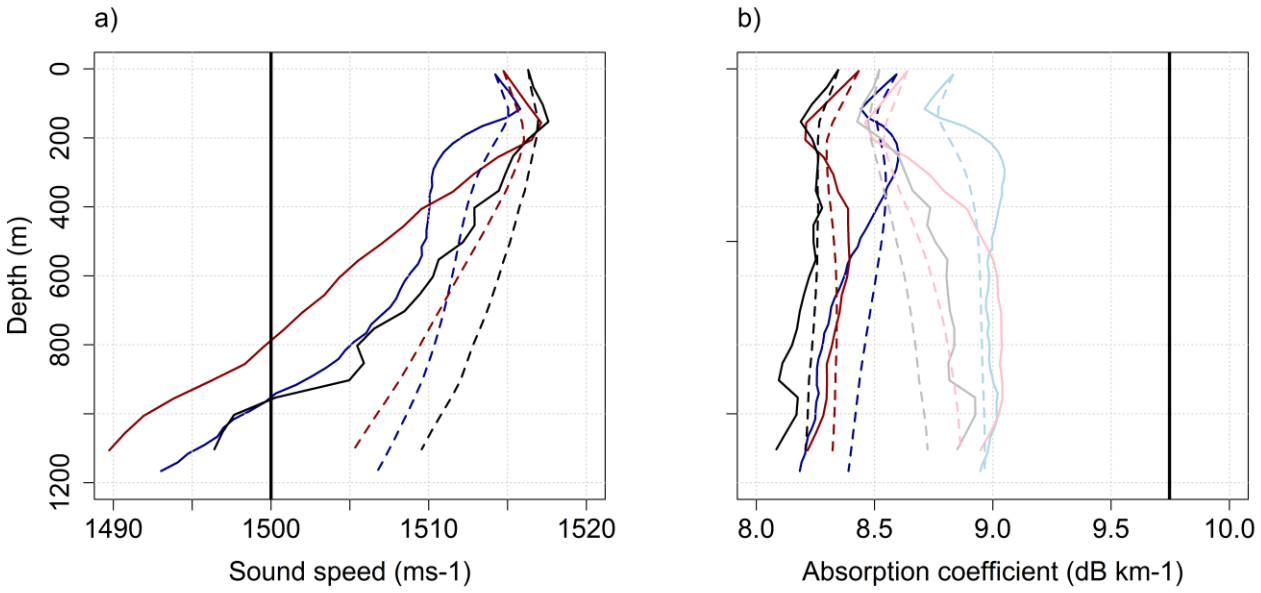

Figure 2.11 Sound speed (a) and absorption coefficient (b) profiles for SB2005 (blue) and SB2009 (red) acoustic surveys of orange roughy and a CTD cast of Sleeping Beauty in 2014 (black and grey). The dashed lines show the cumulative profiles and the solid lines show calculated values. Sound speed is based on equations in Mackenzie (1981) and absorption is based on equations in Doonan *et al.* (2003) (dark colours in b) and Francois and Garrison (1982) (light colours in b). The temperature, salinity and depth profiles for 2005 and 2009 were obtained from the Integrated Marine Observing System (IMOS) online database (see Table 2.3 for details). The solid vertical black line in show nominal sound speed and absorption coefficient used to collect the data.

Table 2.7 Summary of absorption correction factors and cumulative absorption (dB/km) at 1100 m using equations by Francois and Garrison (1982) (F & G) and Doonan *et al.* (2003) (Doonan).

Survey	Correction factor		Cumulative absorption (dB/km) at 1100 m	
	F & G	Doonan	F & G	Doonan
SB2005	0.68	0.52	8.97	8.41
SB2009	0.66	0.51	8.85	8.33

Inference area

The inference area (i.e. survey area) (a_s, in nmi^2) was drawn manually based on the outermost points of the survey transects. The inference polygon was drawn approximately half a transect spacing around the set of observations (each observation represents a 100 m interval). The a_s was then calculated using the geosphere package in R. Once drawn the polygons were saved in both .Rdata and .csv formats so that they could be referred to again in the future. Storing the polygon files removes uncertainty surrounding the redrawing. It is highly recommended that all future analysis store the polygon coordinates in an easily readable format (e.g. .csv or .xlsx).

Target strength to length

The target strength (*TS*, in dB re 1 m^2) to length (*SL*) equation used was taken from the FAO (2017) review which was updated from the Niklitschek and Patchell (2015) for the larger Indian Ocean orange roughy that ranged from 35 to 60 cm. To extrapolate to the larger orange roughy found in the Indian Ocean at 38 kHz, the following *TS* equation of the form *TS*=*a**log10(*SL*)-*b* was proposed:

$$TS=16.37*\log10(\overline{SL_g})-77.17, \quad (\mathbf{2.10})$$

where *a* is the slope derived from McClatchie *et al.* (1999) and *b* is the intercept derived from Kloser *et al.* (2013). For a geometric mean fish length of 44.6 cm this equation gives a *TS* value of -50.17 dB re 1 m^2 at 38 kHz. Using the *TS*-*SL* equation given in Niklitschek and Patchell (2015):

$$TS=16.15*\log10(\overline{SL_g})-76.71, \quad (\mathbf{2.11})$$

gives a *TS* of -50.07 dB re 1 m^2 for the same mean length. Use of the Niklitschek and Patchell (2015) *TS*-*SL* equation would result in a decreased biomass estimate of 2.3%. The effects on *TS* for SB2005 and SB2009 are given in Table 2.8.

Table 2.8 Target strength to length parameters (*a* and *b*) given by [1]McClatchie *et al*. (1999), [2]Kloser *et al* (2013), and [3]Niklitschek and Patchell (2015). Mean geometric standard length ($\overline{SL_g}$, cm) is based on values in given in Table 2.4 (appropriate for each year) assuming a 1:1 sex ratio of male and female.

Survey	*a*	*b*	Mean SL_g (cm)	Mean *TS* (dB re 1 m^2)
SB2005	16.37[1]	77.17[2]	45.80	-49.98
	16.15[3]	76.71[3]		-49.89
SB2009	16.37[1]	77.17[2]	44.65	-50.16
	16.15[3]	76.71[3]		-50.07

Biomass estimation

Vessel-based biomass estimates were made at 38 kHz based on delineated regions that were classified as orange roughy, using corrected acoustic density estimates (corrected for absorption and calibration (for SB2005)). The estimates provided are considered as independent snapshots of the orange roughy population at Sleeping Beauty. Volume backscattering coefficients (s_v, m^2 m^{-3}) from orange roughy aggregations were integrated (nautical area scattering coefficient, s_A in m^2 nmi^{-2}) and averaged over EDSU of 100 m, using standard echo-integration methods (MacLennan *et al*. 2002; Simmonds and MacLennan, 2005). The average s_A ($\overline{s_A}$) for the inference area (a_s, nmi^2) was then calculated (MacLennan, 1990). This along with a_s and estimates of mean population target strength ($\overline{TS}$, dB re 1 m^2) and arithmetic mean population fish weight ($\overline{W_a}$, g) were used to estimate orange roughy biomass. Population sex ratio was assumed to be 1:1 when estimating $\overline{TS}$ and $\overline{W_a}$. It is also assumed that orange roughy contributed 100% of the acoustic energy within the delineated aggregations and zero of the energy outside of the aggregations. The biomass calculation can then be broken in to three parts. Firstly, scatter area density ρ_v (fish/nmi^2) is given as:

$$\rho_v = \overline{s_A}/4 \cdot \pi \cdot 10^{(\frac{\overline{TS}}{10})}. \quad \textbf{(2.12)}$$

From this the scatter abundance (n_b, number of fish) in the a_s is calculated:

$$n_b = \rho_v \cdot a_s. \quad \textbf{(2.13)}$$

Scatter biomass (m_b, tonnes) of fish observed over the entire a_s is then:

$$m_b = n_b \cdot \overline{W_a}/1e\text{-}6. \quad \textbf{(2.14)}$$

Estimation of variance

The associated survey sampling coefficient of variation (CV, %) was calculated using intrinsic geostatistical methods (summarised below, see Scoulding *et al*. 2016 for details) implemented in the R package RGeoStats (Renard *et al*. 2015).

Due to the highly skewed nature of acoustic data (characterised by a large number of zero values and a few very high s_A values) the variograms were derived using a logarithmic transformation of the data (Rivoirard *et al*. 2000). The variogram of the log transformed data was determined according to the classical estimator (Matheron, 1971). The resultant variograms were

backtransformed following the methods described by Guiblin *et al*. (1995). These were subsequently fitted with an exponential model. In order to compute the estimation variance, the survey area was divided into an equally spaced discretisation grid of 50 m for SB2005.1, 60 m for SB2005.2 and 140 m for SB2009. As intrinsic methods (Matheron, 1971) present a much finer description of the spatial structure they are more commonly used to determine estimation variance (Rivoirard *et al*. 2000). The number of discretisation steps used to calculate the mean co-variogram was varied to minimise the estimation variance. The variance of the summed estimation variances was then calculated, followed by the CV (Rivoirard *et al*. 2000).

2.2 Results

Snapshot acoustic biomass estimates for SB2005 and SB2009 are presented below. These surveys were considered to have suitably low bias and error due to species uncertainty, data quality and other sources of error. It was assumed that aggregations were made up of 100% orange roughy, which could be easily delineated from surrounding backscatter. Survey results are given in Tables 2.10 and 2.11. Biomass estimates and s_A means are based on absorption equations given by Doonan *et al*. (2003) and exclude the deadzone. Acoustic density plots for SB2005 and SB2009 are shown in Figures 2.12 and 2.13 respectively.

In 2005 the biomass estimates for SB2005.1 and SB2005.2 were 4,309 and 2,236 tonnes, respectively (Table 2.9), with respective inference areas of 1.11 and 1.68 nmi^2. The deadzone was estimated at 0.25 and 0.05 % for SB2005.1 and SB2005.2, respectively and sampling CV was 8.7 % for SB2005.1 and 5.5 % for SB2005.2 (Table 2.10). In 2009 the biomass estimate was 17,050 tonnes with an inference area of 3.46 nmi^2, a deadzone estimate of 1.03 % and a sampling CV of 11.2 %.

Table 2.9 Analysis of SB2005 acoustic survey of orange roughy. The calibration correction factor applied to s_A values was 1.22. Biomass and s_A mean are based on Doonan *et al*. (2003) equations for absorption and exclude the deadzone component. EDSU = Equivalent distance sampling unit.

	Unit	Survey	
		2005.1	2005.2
EDSU s_A mean above deadzone	m^2 nmi^{-2}	165	57.1
s_A sampling CV	**%**	**8.7**	**5.5**
Inference area	nmi^2	1.11	1.68
Numeric density	fish/m^2	0.52	0.13
Biomass above deadzone	tonnes	4309	2236
Deadzone estimate	%	0.25	0.05
Biomass estimate	**tonnes**	**4320**	**3358**
EDSU distance	m	100	100
Number of EDSU	-	157	155
Number of transects	-	6	5
Mean transect spacing	m	248	387
Geostatistical grid spacing	m	50	60
Aggregations bounded	yes/no	no	No

Table 2.10 Analysis of SB2009 acoustic survey of orange roughy. Biomass and s_A mean are based on Doonan *et al*. (2003) equations for absorption and exclude the deadzone component. EDSU = Equivalent distance sampling unit.

	Unit	Value
EDSU s_A mean above deadzone	m^2 nmi^{-2}	216
s_A sampling CV	**%**	**11.2**
Inference area	nmi^2	3.46
Numerical density	fish/m^2	0.52
Biomass above deadzone	tonnes	17050
Deadzone estimate	%	1.03
Biomass estimate	**tonnes**	**17226**
EDSU distance	m	100
Number of EDSU	-	245
Number of transects	-	10
Mean transect spacing	m	543
Geostatistical grid spacing	m	140
Aggregations bounded	yes/no	yes

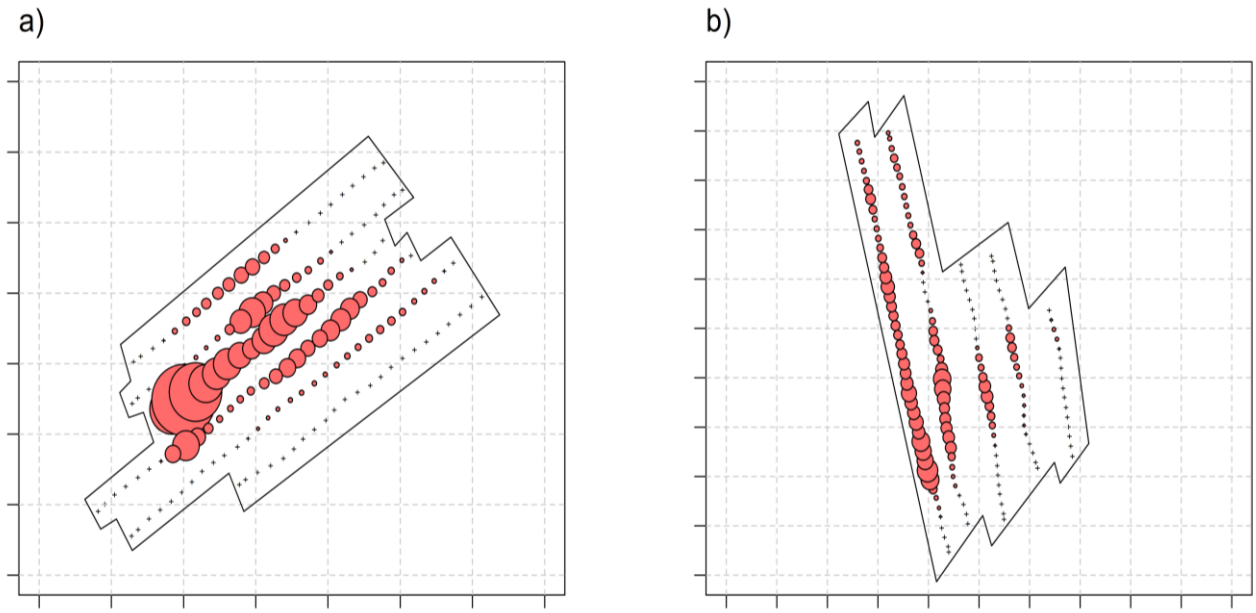

Figure 2.12 Bubble plot representing the average acoustic density (Nautical Area Scattering Coefficient, s_A, in m^2 nautical $mile^{-2}$) of orange roughy by 100 m intervals along the cruise track during the 2005 orange roughy acoustic survey on Sleeping Beauty at 38 kHz for (a) survey 1 (SB2005.1) and (b) survey 2 (SB2005.2). Black crosses show zero s_A. Circle diameter represents linear proportion to area density. The largest s_A observations were 3,588 and 375 m^2 nautical $mile^{-2}$ with a mean acoustic density of 165 and 57 m^2 nautical $mile^{-2}$ for SB2005.1 and SB2005.2, respectively. The black polygons denote the inference area analysed which have areas of 1.11 and 1.68 nmi^2 for SB2005.1 and SB2005.2, respectively. The s_A values have been corrected for calibration and for absorption using the equations given by Doonan *et al*. (2003). The grid is 500 x 500 m.

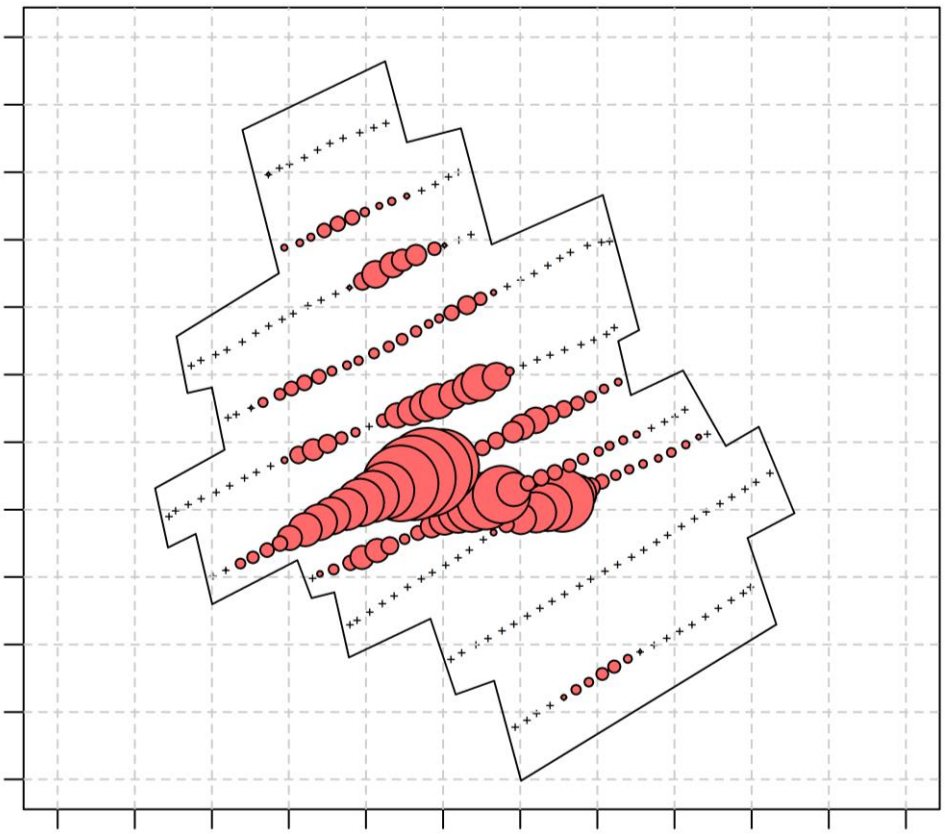

Figure 2.13 Bubble plot representing the average acoustic density (Nautical Area Scattering Coefficient, s_A, in m^2 nautical $mile^{-2}$) of orange roughy by 100 m intervals along the cruise track during the 2009 orange roughy acoustic survey on Sleeping Beauty at 38 kHz. Black crosses show zero s_A. Circle diameter represents linear proportion to area density. The largest s_A observation was 4,656 m^2 nautical $mile^{-2}$ and a mean acoustic density of 261 m^2 nautical $mile^{-2}$. The black polygon denotes the inference area analysed which has an area of 3.46 nmi^2. The s_A are calibrated using calibration values determined in Echoview and corrected for absorption using the equations given by Doonan *et al*. (2003). The grid is 500 x 500 m.

3 Target strength of orange roughy (*Hoplostethus atlanticus*) *in situ*

A data set (hereafter referred to as SB2014) containing Acoustical Optical System (AOS) data was selected to measure the target strength (*TS*, dB re 1 m^2) of orange roughy (standard length, *SL* = 45-60 cm) *in situ*. Acoustic and optical measurements were collected on 4th July 2014 from orange roughy spawning aggregations on Sleeping Beauty (SB) in the south Indian Ocean (Figure 3.1). Biological data was available for SB which was collected between 23rd June and 5th July 2014 and a CTD deployment on SB was made on the 5th July 2014 (see Figures 2.4 and 2.12 for environmental profiles). *In situ TS* measurements were made using Sealords net-mounted AOS, deployed from the FV *Will Watch*. The AOS was attached to the headline of a standard commercial orange roughy demersal trawl (see Ryan *et al.*, 2009 and Kloser *et al.*, 2013 for a detailed description of the AOS). The trawl was towed at a speed of 2-4 knots (1.2-1.7 ms^{-1}) through aggregations of orange roughy. The net was towed across the top of SB at a depth of about 1100 m with the AOS at 2-12 m above the seabed (this applies to the areas where *TS* measurements were made) (Figure 3.2). Target

strength measurements are based on 6 minutes of optically verified acoustic data collected between 01:45-01:51 UTC. Acoustical and optical data were downloaded following the AOS deployment.

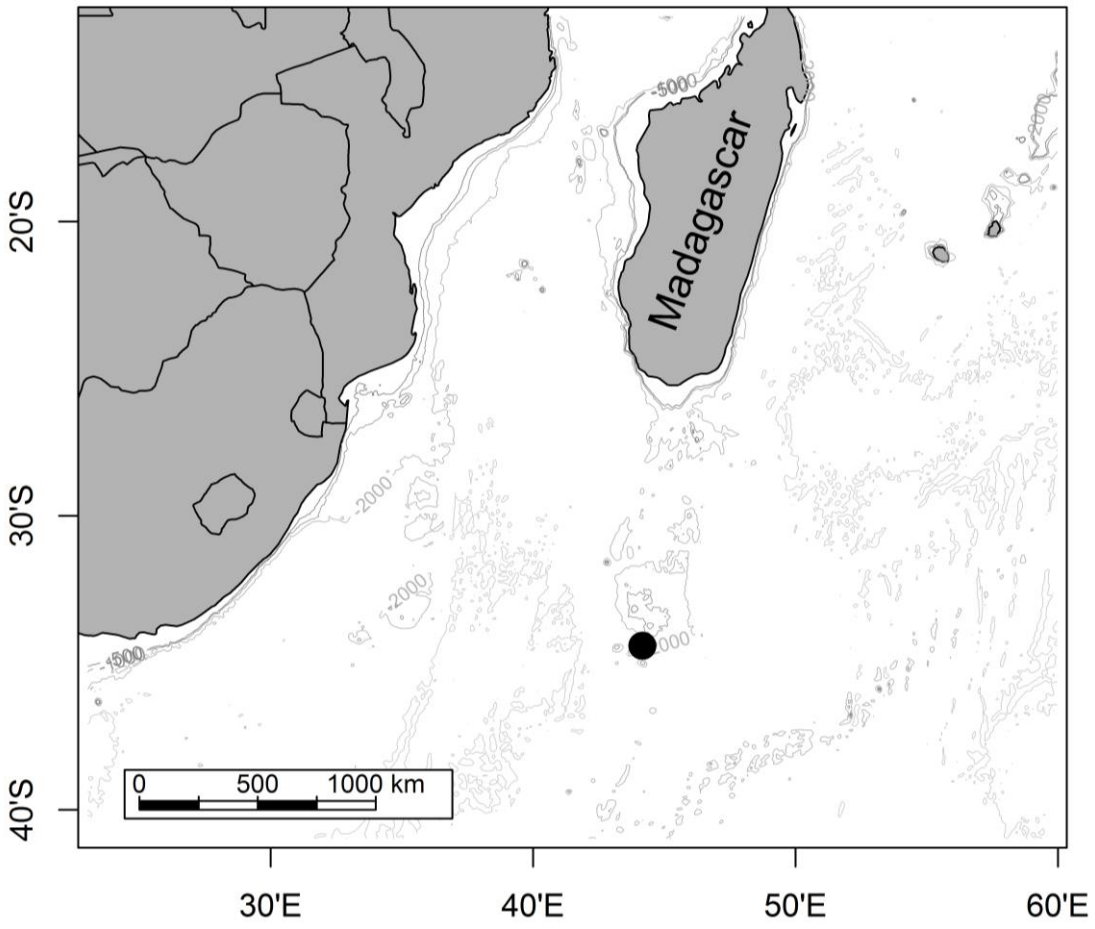

Figure 3.1 Approximate location of the experimental area (filled circle) on Sleeping Beauty fishing ground in the south Indian Ocean, to the south of Madagascar.

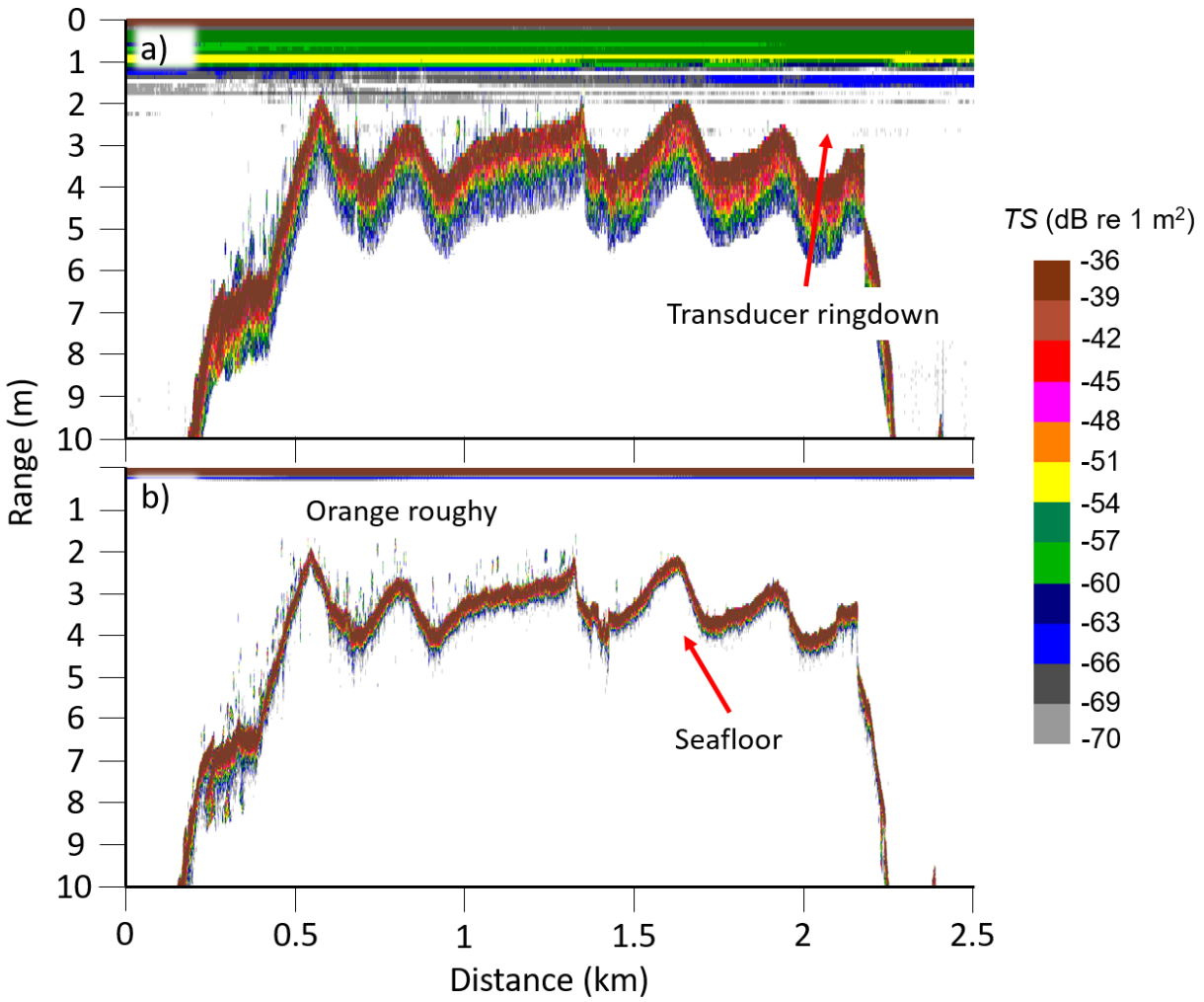

Figure 3.2 Echogram of target strengths (*TS*, in dB re 1 m²) at (a) 38 kHz and (b) 120 kHz from an AOS pass over Sleeping Beauty fishing ground.

3.1 Materials and methods

3.1.1 Data

Acoustic data

The AOS houses two Simrad EK60 echosounders, 38 and 120 kHz (Figure 3.3), respectively connected to Simrad 38 kHz ES38-DD and Simrad 120 kHz ES120-7D split-beam transducers, with nominal 3 dB beamwidths of 7°. Echosounder details and recording parameters are given in Table 3.1. Using the centre of the 38 kHz transducer as the reference, the 120 kHz acoustic data were offset in Echoview by -390 mm in the along-track direction to make the acoustic samples spatially comparable. No offset was required in the across-track direction as the instruments were aligned.

Two additional transducers were also housed on the AOS (12 and 200 kHz) but neither were used in this analysis (Figure 3.3). A ship-mounted Simrad ES60 38 kHz echosounder was concurrently operated during the deployment of the AOS but the data was also not analysed here and did not appear to interfere with the echosounder on the AOS. However, a net-mounted acoustic sensor does cause high levels of interference with the AOS EK60 38 kHz (seen as irregularly spaced impulse

noise of various intensity), although the effects are only visible on *TS* gain echograms at a range beyond 15-20 m. This is not a problem as the *TS* measurements are made at ranges between 2 and 12 m.

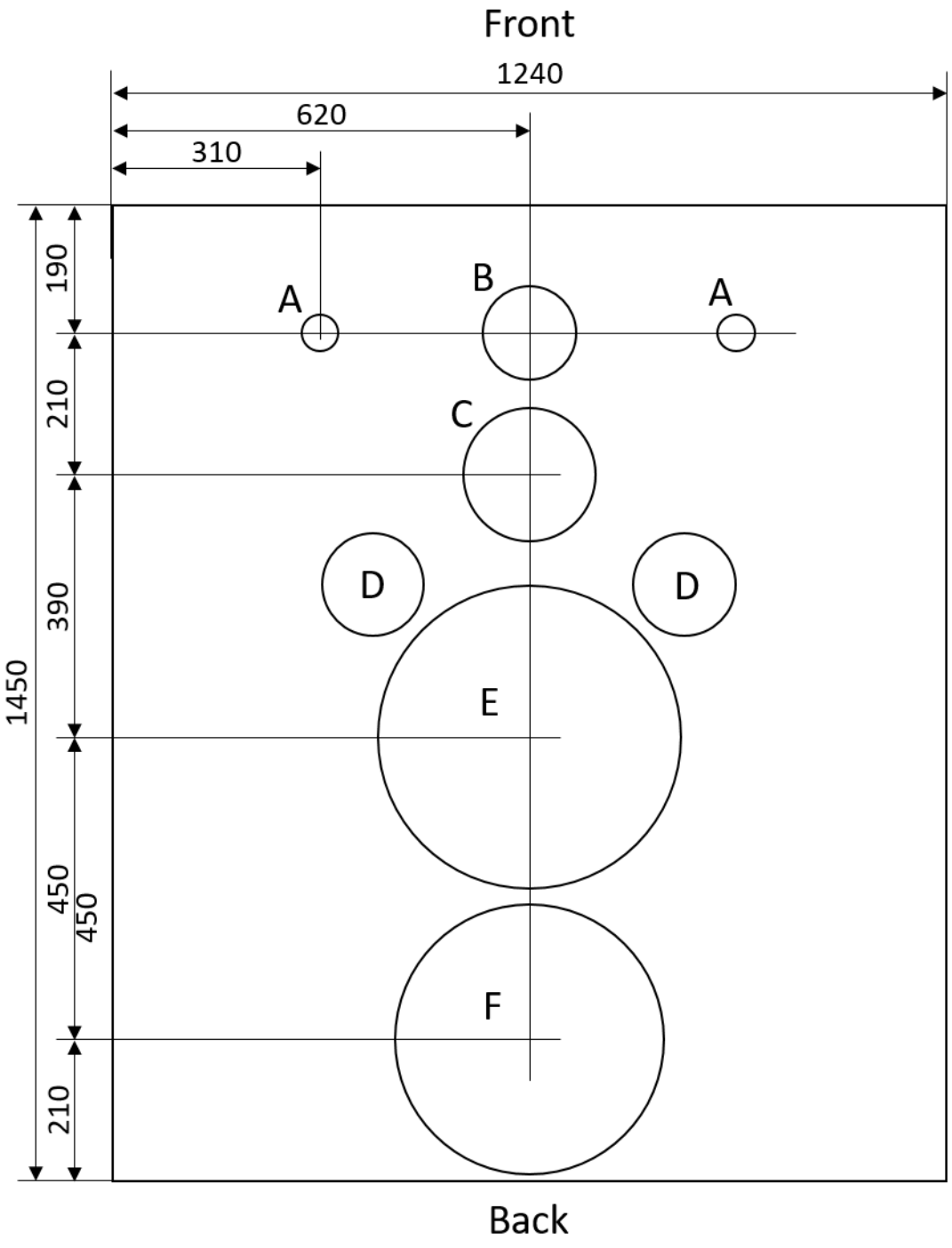

Figure 3.3 Plan view of the acoustic optical system base plate showing the locations of (a) lasers, (b) video camera, (c) 120 kHz transducer, (d) lighting, (e) 38 kHz transducer and (f) 12 kHz transducer.

Table 3.1 Echosounder parameters and settings.

Parameter	Unit	Value	
Frequency	kHz	38	120
Transducer model	-	Simrad ES38-DD	Simrad ES120-7CD
Transducer serial number	-	28363	115
Transceiver serial number	-	0090720179e5 1	009072073bbe 1
Power	W	2000	500
Pulse duration	ms	2.048	1.024
Beamwidth -3 dB power	°	7	7
Two-way beam angle	dB re 1 sr	-20.5	-21.0
Nominal sound speed	ms^{-1}	1500	1500
Nominal absorption coefficient	dB km^{-1}	9.97	37.31
Nominal gain	dB re 1	25.5	27.0
Nominal s_a correction	dB re 1	0.00	0.00
Calibrated gain	dB re 1	23.45	27.87

Echosounder calibration

The echosounders were calibrated at depth by lowering and retrieving the AOS (when removed from the trawl net) slowly and holding it in place at three discrete depths of 600, 800 and 1000 m with a 38.1 mm tungsten carbide sphere (theoretical *TS* at 1000 m = -42.4 dB re 1 m^2 at 38 kHz and -39.48 dB re 1 m^2 at 120 kHz) suspended ~20 m below the transducers to give a calibration that compensated for the variation in transducer performance with depth (Ryan *et al.*, 2009). The calibration was performed in Echoview Version 8.0.92 and the calibration results are given in Table 3.2. Compensated targets strength measurements showed a flat response across the beam width (Ryan and Cordell, 2014). As the AOS was deployed ~1100 m the calibration values used were based on measurements made at 1000 m.

Table 3.2 Relevant calibration settings and environmental parameters used in Echoview at 1000m depth.

Parameter	Unit	Value	
Frequency	kHz	38	120
Power	W	2000	500
Pulse duration	ms	2.048	1.024
Calibrated gain	dB re 1	23.45	27.87
Angle sensitivity (both axis)	electrical°/geometric°	22.00	23.00
Beamwidth -3 dB power	°	7	7
Sound speed	ms^{-1}	1497.9	1497.9
Absorption coefficient	dB km^{-1}	8.8649	30.327

Optical data

In addition to the echosounders the AOS also comprised of a Hitachi HV-D30P video camera (see Table 3.3 for details), two LED light arrays, two red lasers (not working during the SB2014 deployment) (Figure 3.3, see Ryan et al., 2009 for further details), as well as, an attitude sensor, batteries, control systems and data storage units. The video footage was used to verify acoustically detected targets.

Table 3.3 AOS video camera specifications.

Parameter	Description
Make	Hitachi
Model	HV-D30P
Lens	Fujinon 2.8 mm lens
Lens angles of view	59° in water (horizontal)
Optical system	3° x 1/3" CCD, colour
Aperture	F2.2
Imaging system	R, G, B 1/3 inch CCD
Resolution	752 x 582 (effective pixels = 437,664)
Framesize	Diagonal = 6.0 mm Width = 4.8 mm Height = 3.6 mm
Focal length	2.8 mm
Focal length multiplier	1
Format	PAL
Lighting	Two 60-W LED arrays

Biological data

Biological data was available from Sleeping Beauty fishing ground. Length, sex, stage of maturity, weight and gonad weight measurements were made for 698 orange roughy between the 23rd June and 5th July 2014. Females had a $\overline{SL_g}$ of 46.2 cm (1 SD 3.1 cm) and males had a $\overline{SL_g}$ of 42.7 cm (1 SD 3.2 cm) (Table 2.4).

Environmental data

Sound speed and acoustic absorption were calculated using MacKenzie (1981) and Francois and Garrison (1982) formulas, respectively, using data from a CTD deployment on SB on 5th July 2014 (see Figures 2.4 and 2.12 for depth profiles). The equations were implemented using the R programming software (R core team, 2017). Data were recorded from the surface down to 1145 m. At a depth of 1100 m (the average depth at which target strength measurements were made) the environmental parameters were: temperature = 7.44 °C, salinity = 34.54 psu, sound speed = 1497.9 ms^{-1}, absorption at 38 kHz = 8.86 dB km^{-1} and absorption at 120 kHz = 30.24 ms^{-1}. These values were input in Echoview for acoustic processing (Table 3.2).

3.1.2 Analysis

The acoustic data were processed and the calibration (namely system gain) and environmental (namely sound speed and absorption coefficient) values were applied in Echoview (version 8.0.86, Echoview Software Pty Ltd, Hobart, Tasmania) (Table 3.2). The basic analysis steps are depicted in Figure 3.4 and briefly described below.

A combination of *TS* (Figures 3.4a and 3.4b), single target (Figures 3.4c and 3.4d), angular (location in beam) and optical information (Figure 3.5) were used to confirm target selection. Once a target was verified a rectangular region was drawn around it which was then manually altered to encompass the targets (Figures 3.4e and 3.4f) and masked to exclude all non-verified targets or targets that were not sufficiently separated.

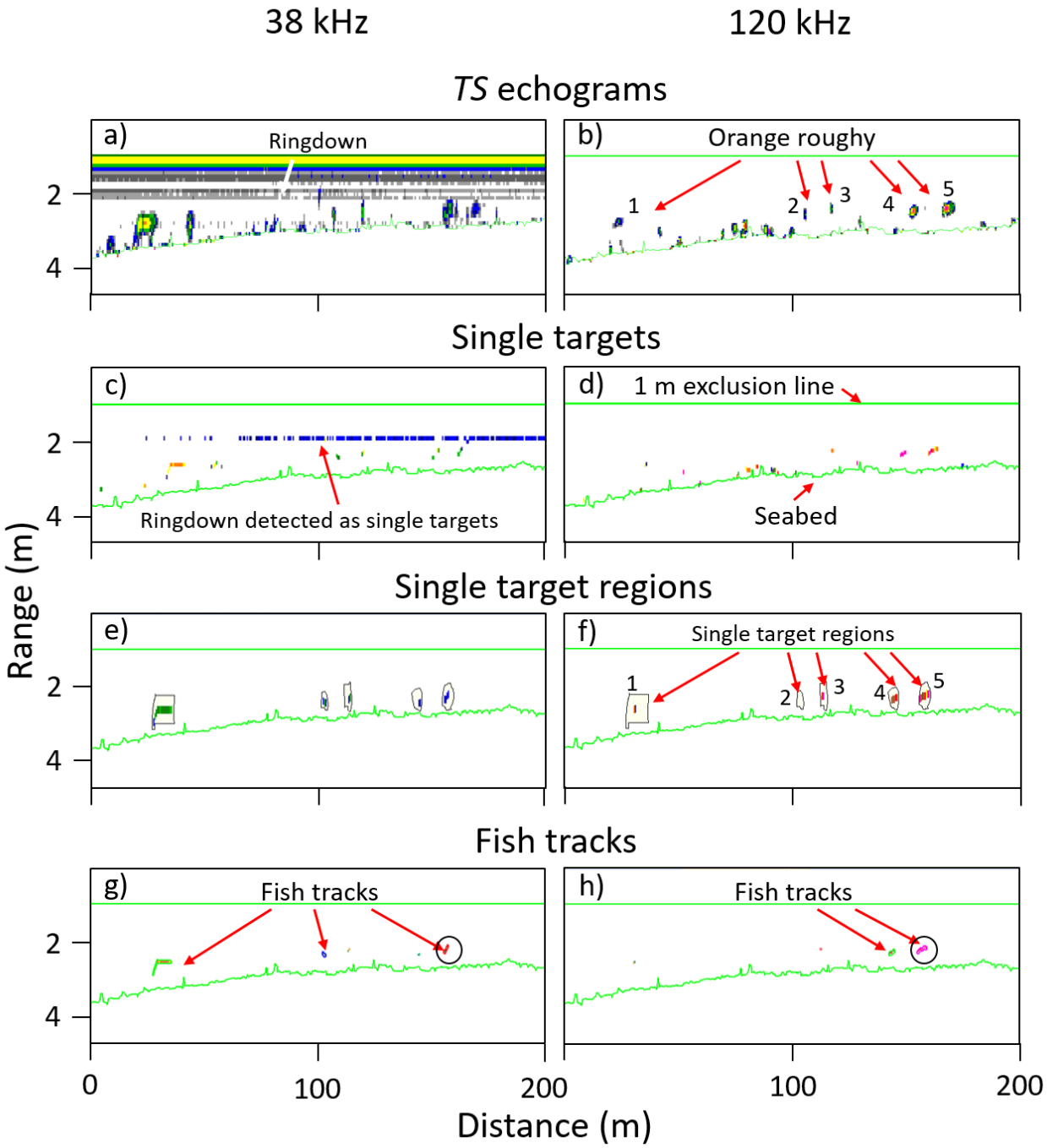

Figure 3.4 Echoview analysis steps showing *TS* echograms at (a) 38 kHz and (b) 120 kHz, single target echograms at (c) 38 kHz and (d) 120 kHz using the settings given in Table 3.4, masked single target echograms (i.e. with all non-verified orange roughy targets removed) with regions (black polygons) showing verified orange roughy targets at (e) 38 kHz and (f) 120 kHz and fish tracks detected at (g) 38 kHz and (h) 120 kHz using the settings in Table 3.4. Regions denoted 1-5 in b and f correspond to the screenshots shown in Figure 3.5. The colour scale is S_v (in dB re 1 m^{-1}) in a and b and target strength (in dB re 1 m^2) in c-h, thresholded from -36 dB (brown) to -70 dB (grey). The black circles in g and h represent an orange roughy tracked at 38 and 120 kHz.

Video footage

The video footage was synched to the acoustic data using the time-stamp common to both the acoustic and video datasets (an offset was not required) (Figures 3.4 and 3.5). Acoustically detected targets were only considered for analysis if they could be visually verified by the video footage. Species identification was established by manual inspection of the video images that corresponded to acoustic fish tracks. Based on inspection of the video, data from orange roughy

that were actively diving were excluded from the analysis as their tilt angle was assumed not to be representative of an undisturbed spawning aggregation. It is noteworthy that very few orange roughy appeared to react negatively to the trawl or lights at the distance of measurements.

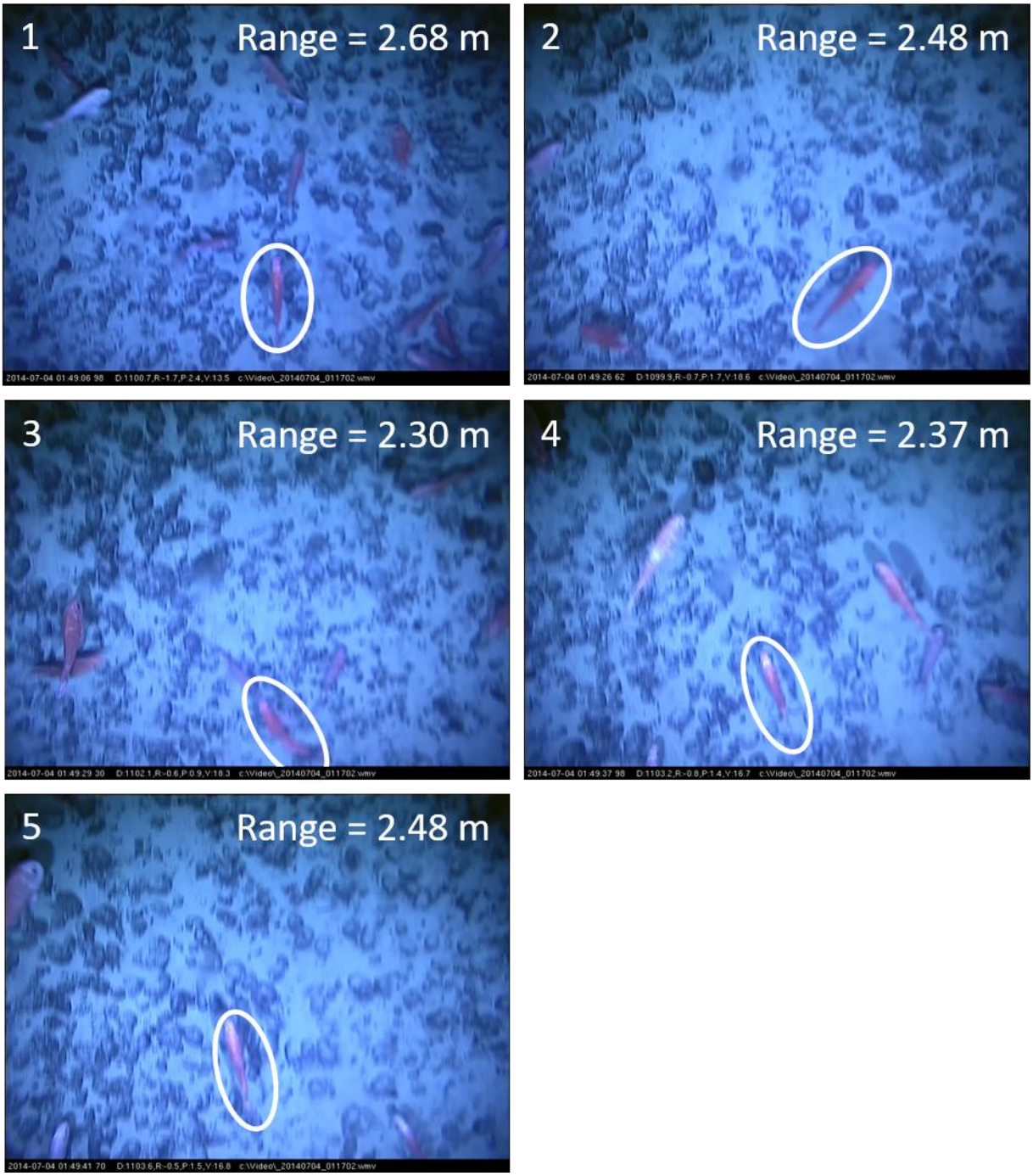

Figure 3.5 Screenshots showing optically recorded orange roughy (white ovals) which are consistent with acoustic measurements. The numbers 1-5 correspond with the regions numbered 1-5 on Figure 3.4.

Single target detection

Target strengths of fish were derived at 38 and 120 kHz data using the single selection criteria given in Table 3.4. A minimum *TS* threshold of -65 dB re 1 m^2 was used at 38 kHz to avoid the erroneous detection of low value targets due to an inferred noise limit (largely caused by the ringdown effect, Figure 3.4a). A minimum *TS* threshold was not necessary for 120 kHz, however, a threshold of -65 dB re 1 m^2 was still used. Targets closer than 2 m to the transducer at either

frequency were excluded from analysis. This was in combination due to the ring down observed at 38 kHz, beam width and near-field effects (see below).

Target tracking

Single targets were used as input to Echoview's fish tracking algorithm (an alpha-beta coefficient filtering model, Blackman, 1986) using the settings given in Table 3.4. For orange roughy tracked at 38 and 120 kHz, the mean *TS* and the logarithmic difference was calculated. The ability to track orange roughy at both frequencies is dependent on range, beam overlap and position within the beam.

Table 3.4 Single target detection and fish tracking settings.

Parameter	Unit	Value	
Frequency	kHz	38	120
Single target detection settings			
TS threshold	dB re 1 m^2	-65	
Pulse length determination level	dB re 1 m^2	6	
Minimum normalised pulse length	-	0.3	
Maximum normalised pulse length	-	1.5	
Maximum beam compensation	dB	12	
Maximum phase deviation minor axis	°	3	
Maximum phase deviation major axis	°	3	
Fish tracking settings			
Alpha	-	0.7	
Beta	-	0.5	
Minimum number of single targets	-	3	
Minimum number of pings	-	3	
Maximum gap between single targets	-	1	

Echoview exports

Single targets and fish tracks at 38 and 120 kHz were exported from Echoview as .csv files. Important single target export data consists of compensated target strength values, target range, alongship and athwartship angles in beam, and ping time. Key fish track exports include mean compensated target strength, mean target range, number of targets in the track and ping times. Together this information can be used to further verify the useability of the detections. Exports were further analysed using the programming language R (R core team, 2017).

3.1.3 Considerations for measuring target strength

The minimum acceptance range of a target is considered with respect to:

1) the transducer near-field,
2) the fish-near-field,

3) the range at which a target is fully ensonified in the beam (i.e. when a target becomes a point scatterer rather than a volume scatterer), and
4) separation distance.

Kloser *et al*. (2013) and Macaulay *et al*., (2013) set a minimum acceptance range of 3 m for orange roughy single targets (mean *SL* = 35 cm). This was estimated to be 1.1 and 3.44 times greater than the near-field of the 38 and 120 kHz transducers, respectively. Kloser *et al*. (2013) estimated the near-field of a 35 cm orange roughy to be 0.5 and 1.5 m at 38 and 120 kHz, respectively. Here, we describe the methods used to calculate the near-field of the transducer and the target.

Transducer near-field

The region directly in front of the transducer face, where wave-fronts generated by the transducers individual elements are out of phase (i.e. not parallel), is referred to as the near-field. In this region the intensity varies rapidly with range. It is only in the far-field, where the element wave-fronts are nearly parallel, that the beam is properly formed and the inverse square law applies (Simmonds and MacLennan, 2005). It is recommended that target strength measurements be made outside of the near-field to apply the inverse square law. A commonly used transducer near-field (r_{nf}, m) equation, is given in Simmonds and MacLennan (2005), as:

$$r_{nf} = \frac{{d_t}^2}{\lambda}, \tag{3.1}$$

where d_t is the linear distance across the transducer face (m) and λ is the acoustic wavelength (m) given as:

$$\lambda = \frac{c_w}{f}, \tag{3.2}$$

where c_w is sound speed in water (ms^{-1}) and f is frequency (Hz). This simple r_{nf} calculation gives an approximation of the range to the near- and far-field boundary. Demer *et al*. (2015) describe a way to estimate d_t from the transducer beamwidth, θ_{-3dB} (in radians (convert from degrees to radians as: radians = degrees*π/180)), using:

$$d_t \cong \frac{3.2}{k\sin(\frac{\theta_{-3dB}}{2})}. \tag{3.3}$$

where the wavenumber k (m^{-1}) is computed as:

$$k = \frac{2\pi}{\lambda}. \tag{3.4}$$

Given some of the uncertainty around the near-field calculation it is common to use a conservative distance of two-threefold (Medwin and Clay, 1998; Simmonds and MacLennan, 2005) the r_{nf} when

carrying out analysis. Based on equations 2.1 to 2.4, recommendations for target analysis based on the approximate r_{nf} for the 38 and 120 kHz installed on the AOS system are given in Table 3.5. Given that twice the near-field at 38 kHz (5.74 m) would exclude almost all single-targets it was necessary to explore if there was a bias between *TS* and range (see results). Figure 3.6 demonstrates how near-field changes as a function of transducer beamwidth and frequency.

Table 3.5 A summary of the near-field parameters for the 38 and 120 kHz transducer installed on the AOS.

Definition	Symbol	Unit	Frequency (kHz)	
			38	120
Transducer	-	-	ES38-CD	ES120-7CD
Beamwidth	Θ_{-3dB}	°	7	7
Sound speed	c_w	ms^{-1}	1500	1500
Wavelength	λ	m	0.039	0.0125
Wavenumber	k	m^{-1}	159	503
Linear distance across transducer face	d_t	m	0.33 (0.48*)	0.10 (0.195*)
Active radius of transducer elements	r_t	m	0.16	0.05
Near-field	r_{nf}	m	2.74	0.87
Twice the near-field	r_{nf}	m	5.48	1.74

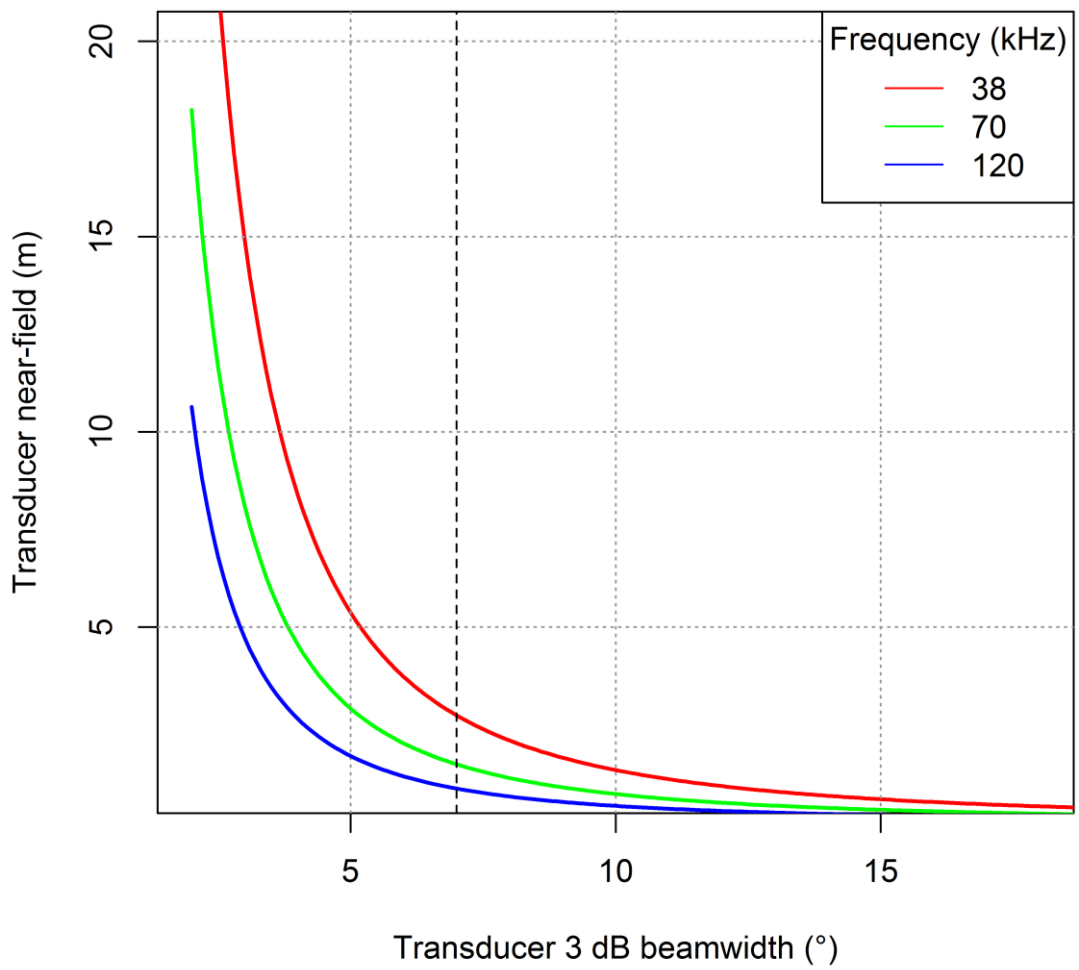

Figure 3.6 Changes in near-field [= 2·r_{nf}, as calculated using Equations 2.1 to 2.4] with transducer -3 dB beamwidth, θ_{-3dB}, at 38 kHz (red), 70 kHz (green) and 120 kHz (blue), for a circular-piston transducer and water sound speed, c_w = 1500 ms^{-1}. The vertical black dashed line shows the near-field ranges for a 3 dB beamwidth of 7°.

Fish near-field

As well as the fish being outside the transducers near-field, the transducer must also be outside of the fish's near-field (Kloser *et al.*, 2013; Demer *et al.*, 2015). However, the acoustic near-field of fish is poorly understood. To estimate r_{nf} for the fish (f_{nf}) we assumed that they approximate an elliptical transducer as:

$$f_{nf} = \frac{SL}{2} \cdot \frac{W_f}{2} \cdot \frac{\pi}{\lambda'}, \quad \textbf{(3.5)}$$

where W_f is the width (cm) of an orange roughy calculated as SL*0.20 (Kloser *et al.*, 2013; Macaulay *et al.*, 2013). The near-field of orange roughy with a standard length frequency distribution of 35-65 cm at 38, 70 and 120 kHz is shown in Figure 3.7. The near-fields of a 45 cm orange are 0.81 and 2.54 m at 38 and 120 kHz, respectively. This assumes that the effective scattering length (the part of the fish that is responsible for >90% of the backscatter) is equivalent to the standard length. In this example it is assumed that SL is the appropriate length, which is

considered acceptable as a guide but depending on fish shape (morphology) and internal composition the effective length may be different.

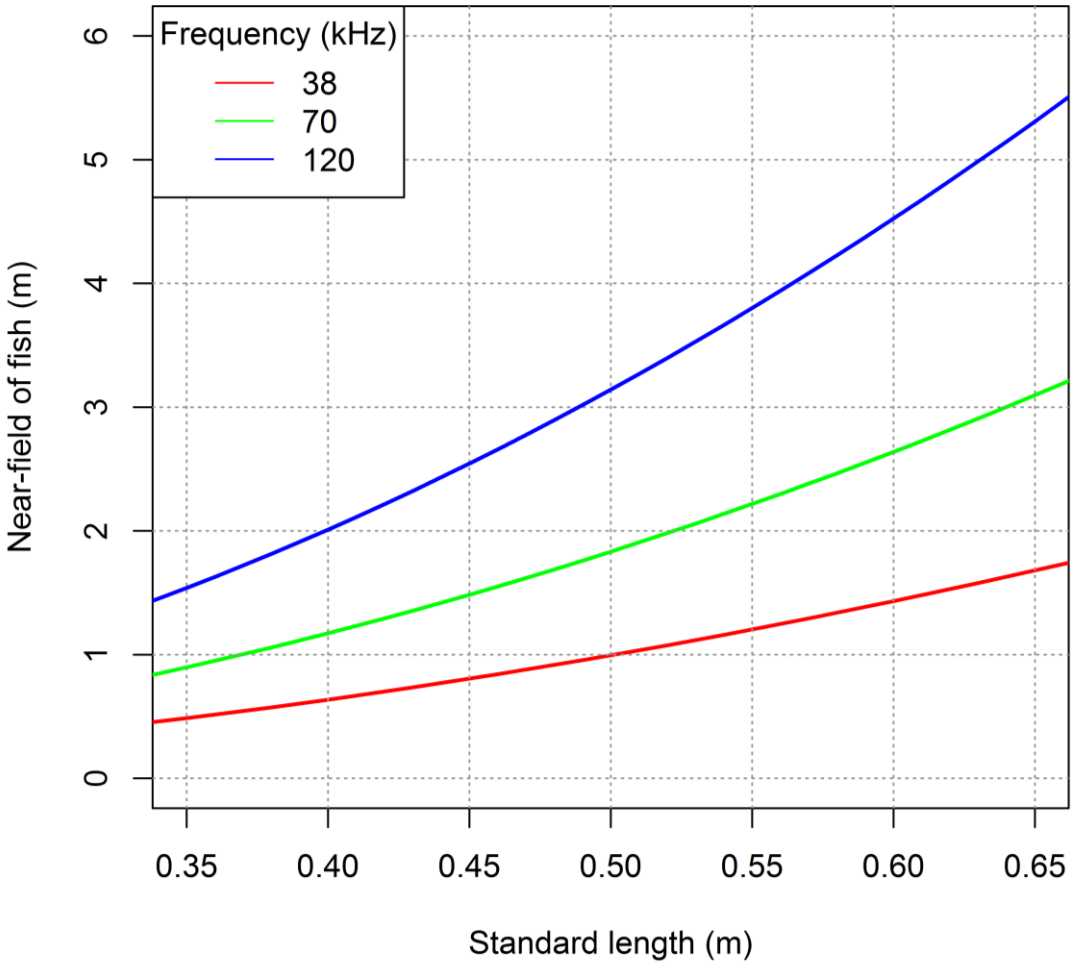

Figure 3.7 Near-field for different sized fish at 38 kHz (red), 70 kHz (green) and 120 kHz (black) with a sound speed of 1500 ms^{-1}.

Point scatterer

The fish must also approximate a point target, which means the beam diameter must be large compared to the major axis of the fish (i.e. *SL*) at the measurement range. To determine this we firstly need to calculate the beam radius d_{rad} (m) as:

$$d_{rad} = \frac{\tan\left(0.5\left(\frac{\theta_{-3dB}\pi}{180}\right)\right)r \cdot 2}{2}, \quad (3.6)$$

where r is range (m) of the fish. It can also be informative to look at the beam area A_{beam} at a given range which is simply:

$$A_{beam} = \pi {d_{rad}}^2. \quad (3.7)$$

Changes in beam diameter (d_{rad}·2) with range are shown in Figure 3.8. An on-axis fish with a mean *SL* of 45 cm must be ~ 3.7 m from the transducer (beamwidth = 7°) face to be fully ensonified (Figure 3.9). If the centre of the fish (i.e. half the major axis or *SL*) is off-axis (i.e. not on the acoustic axis) the range will increase. To this end only targets close to the acoustic axis should be considered when measuring *TS* (unless the range is sufficiently large), otherwise it is unclear which part of the fish is responsible for the measured backscatter.

As evidenced in the results this could be problematic for the SB2014 dataset as very few targets were detected on or close to the acoustic axis at a sufficiently large range.

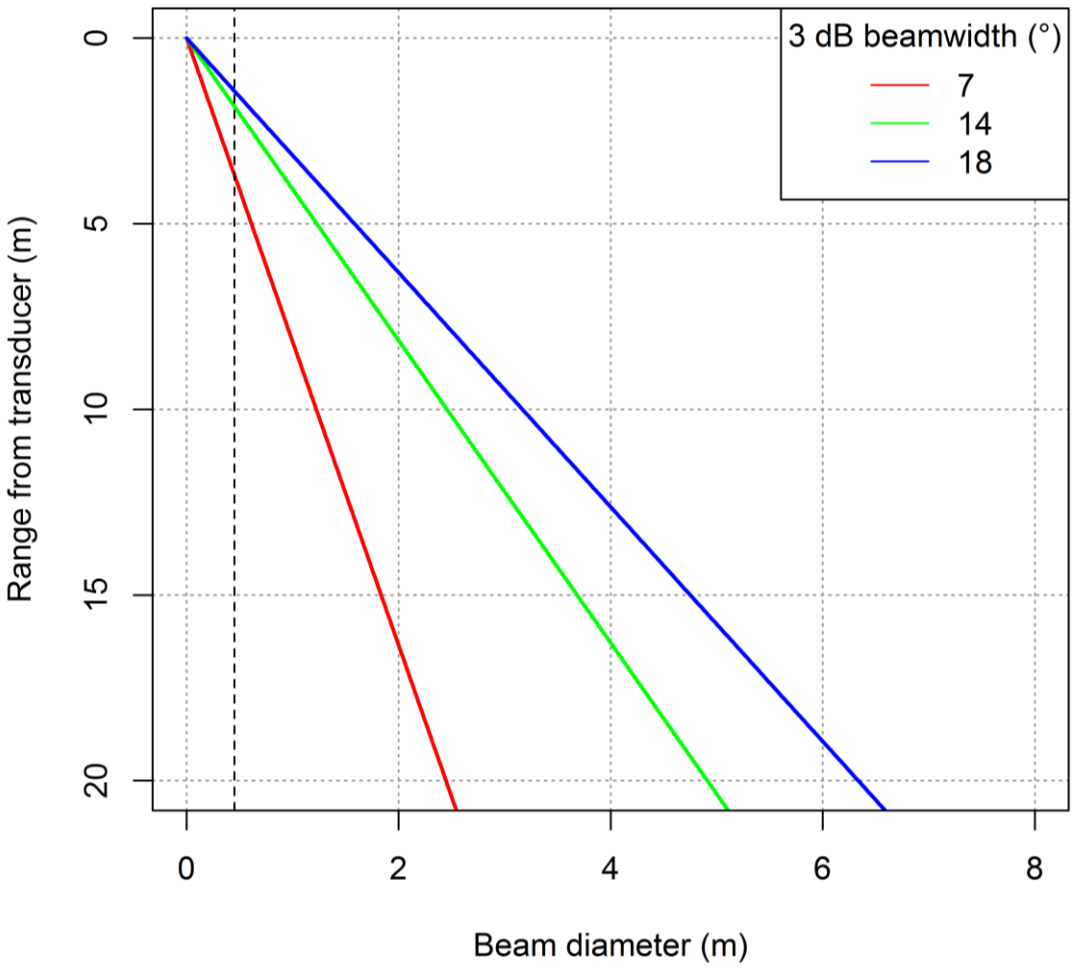

Figure 3.8 Changes in beam diameter (m) with range (m) for three transducer 3 dB beamwidths (°); 7 (red), 14 (green) and 18 (blue). The vertical black dashed line is the mean standard length (m) of an orange roughy from the south Indian Ocean and indicates the range from the transducer at which a fish changes from being a volume scatterer to a point scatterer if on the acoustic axis (see Figure 3.9 for a further example).

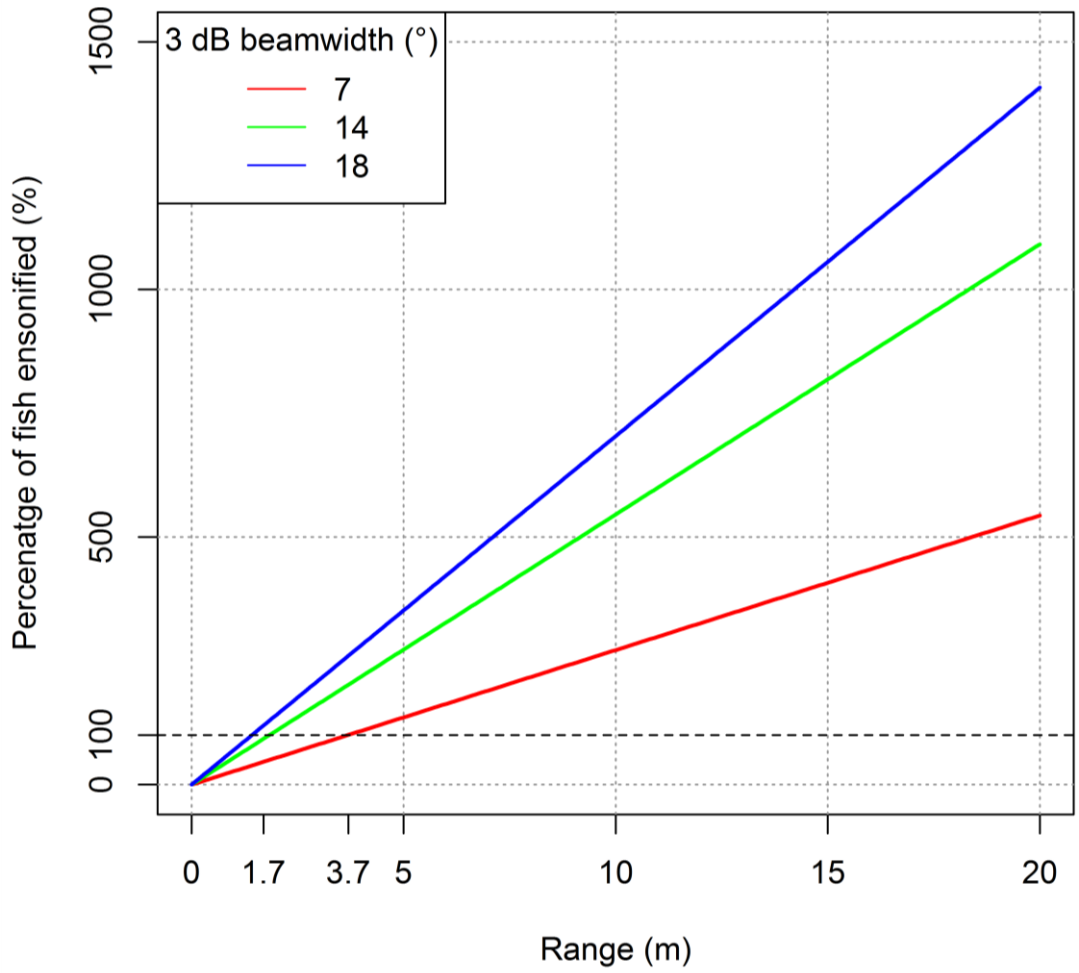

Figure 3.9 Percentage of an orange roughy with an assumed standard length of 44.7 cm ensonified by the acoustic beam with beamwidths of 7° (red), 14° (green) and 18° (blue) at range (m). In this scenario it is assumed that the fish is on the acoustic-axis. The horizontal black dashed line indicates the range at which the fish is 100% ensonified by the beam which corresponds to approximate ranges of 3.7 m for a 7° beamwidth and 1.7 m for 14 and 18° beamwidths.

Target separation

In order for two fish in close proximity to be acoustically resolvable they must be separated by:

$$res = \frac{c_w \tau}{2} + 0.5 H_f, \quad \textbf{(3.8)}$$

where H_f is the height of the fish (m). Here, orange roughy height is assumed to be 46% of the standard length (McClatchie and Ye, 2000). The required separation distances for a range of standard fish lengths and pulse durations is given in Figure 3.10. At the pulse durations used in this report (2.048 ms at 38 kHz and 1.024 ms at 120 kHz) and a c_w of 1500 ms^{-1}, two fish with *SL*'s of 45 cm would have to be separated by 1.64 and 0.87 m at 38 and 120 kHz respectively to be acoustically resolvable. These distances can be difficult to achieve in dense spawning aggregations of orange roughy. For future deployments of the AOS it is recommended that pulse duration is kept as short as possible. Furthermore, pulse durations should be identical when multiple frequencies are used.

This makes spatial comparisons of acoustic samples collected at multiple frequencies easier. However, use of different pulse lengths at high frequencies can be useful.

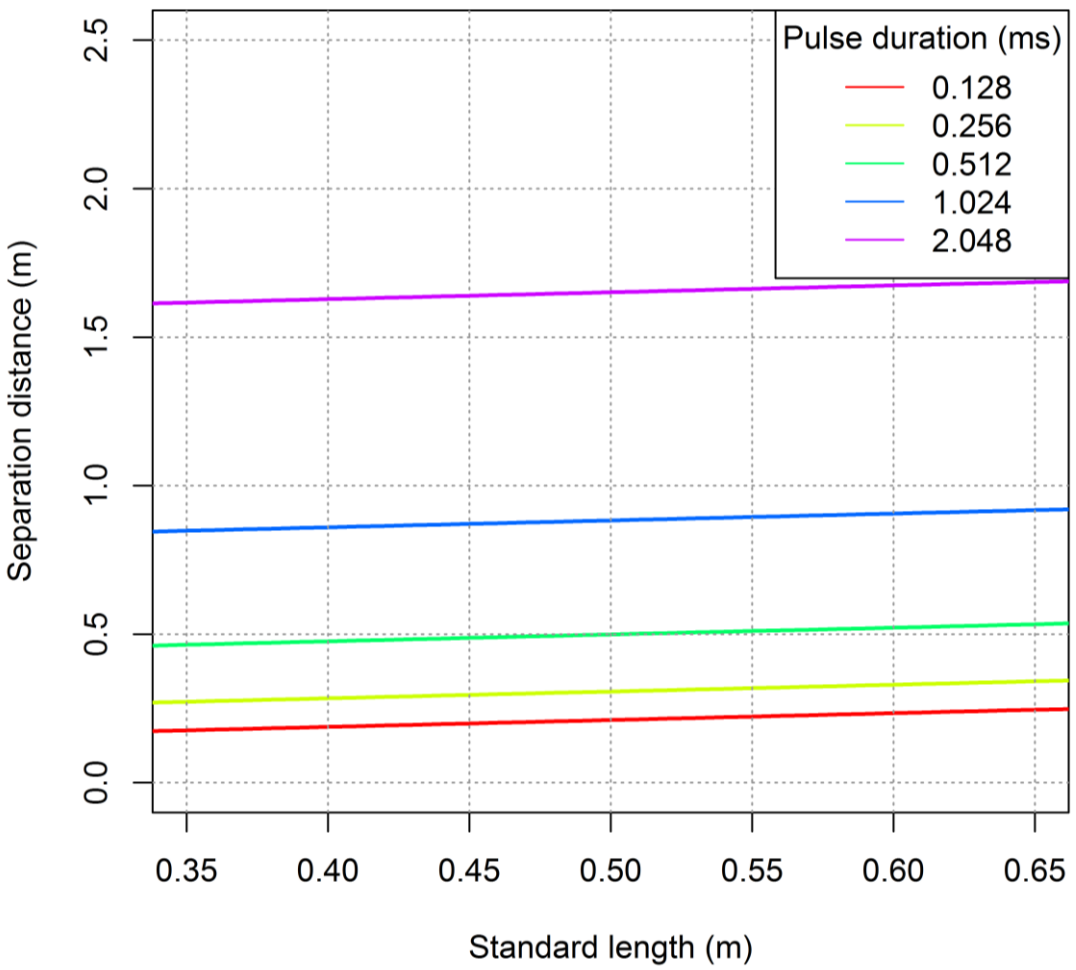

Figure 3.10 Separation distance required for two fish to be resolvable from one another at a number of pulse durations with a sound speed of 1500 ms^{-1}. A range of standard lengths are presented.

3.2 Results

The net-attached AOS, was towed at a depth of around 1100 m, between 2-12 m above the seabed. The only species observed on the video footage was orange roughy which gives high confidence that the single targets and fish tracks originated exclusively from orange roughy. Only fish which could be visually verified were considered for analysis. The transducer near-fields at 38 and 120 kHz are 2.74 m and 0.87 m, respectively. The near-fields of a 45 cm orange roughy are 0.81 and 2.54 m at 38 and 120 kHz, respectively. The minimum acceptance range should be considered with respect to which ever near-field range is greatest. For example the transducer near-field at 38 kHz is greater than the fishes near-field at 38 kHz and should therefore be used (the opposite is true for 120 kHz). If we conservatively consider twice the near-field as the most appropriate minimum acceptance range, then we get minimum acceptance ranges of 5.48 m at 38 kHz and 5.08 m at 120 kHz, which are conveniently similar to one another. Although these conditions may be considered to be the ideal, very few single targets or fish tracks were detected at these ranges in the current study. At

once and twice the near-field only 41 and 18 would be accepted at 38 kHz and 56 and 26 at 120 kHz (Table 3.6). In order to maintain a sufficient number of single targets and fish tracks for analysis we consider all targets >3m away from the transducer.

3.2.1 Single targets

The single target detections (at ranges greater than 3 m) consisted of 14 and 11 optically verified fish at 38 and 120 kHz, respectively. At 38 and 120 kHz, 38 and 43 single targets were detected at a range greater than 3 m, which resulted in mean *TS* of -48.11 dB re 1 m^2 and -45.07 dB re 1 m^2 at 38 and 120 kHz, respectively (Table 3.6). The *TS* distributions are shown in Figure 3.11. The dB difference between 38 and 120 kHz was 3.04 dB re 1 m^2 (Table 3.6), with 120 kHz being the stronger frequency, which is in line with the ~3 dB commonly observed for orange (Ryan *et al.*, 2016). Targets were randomly distributed within the beam (Figure 3.12) and at various depths between 2.2 and 7.6 m at 38 kHz and 2.01 and 7.74 m at 120 kHz (Figure 3.13a). Target strength varied from -60.72 to -41.90 dB re 1 m^2 at 38 kHz and from -59.93 to -37.63 dB re 1 m^2 at 120 kHz (Figure 3.13b).

Twenty six single targets were matched by ping number at 38 and 120 kHz, giving mean *TS* of -48.12 and -45.08 dB re 1 m^2 for 38 and 120 kHz respectively, which gives a mean dB difference of 3.04 dB re 1 m^2 (Figure 3.13c), which is identical to the mean dB difference of all targets detected at ranges greater than 3 m.

Table 3.6 Summary of target strength values using different acceptance ranges. All = all single targets included, $1 \cdot r_{nf}$ = single targets detected at a range greater than once the largest near-field (i.e. transducer near-field at 38 kHz and fish near-field at 120 kHz), $2 \cdot r_{nf}$ = single targets detected at a range greater than twice the largest near-field and >3m = only single targets greater than 3m in range (highlighted in red). N is number of targets.

Frequency (kHz)	All		$1 \cdot r_{nf}$		$2 \cdot r_{nf}$		>3 m	
	Mean *TS* (dB re 1 m^2)	N	Mean *TS* (dB re 1 m^2)	N	Mean *TS* (dB re 1 m^2)	N	Mean *TS* (dB re 1 m^2)	N
38	-48.82	68	-48.32	41	-46.63	18	-48.11	38
120	-46.63	100	-45.48	56	-45.07	26	-45.07	43
dB difference (120 – 38 kHz)	2.19		2.83		1.56		3.04	

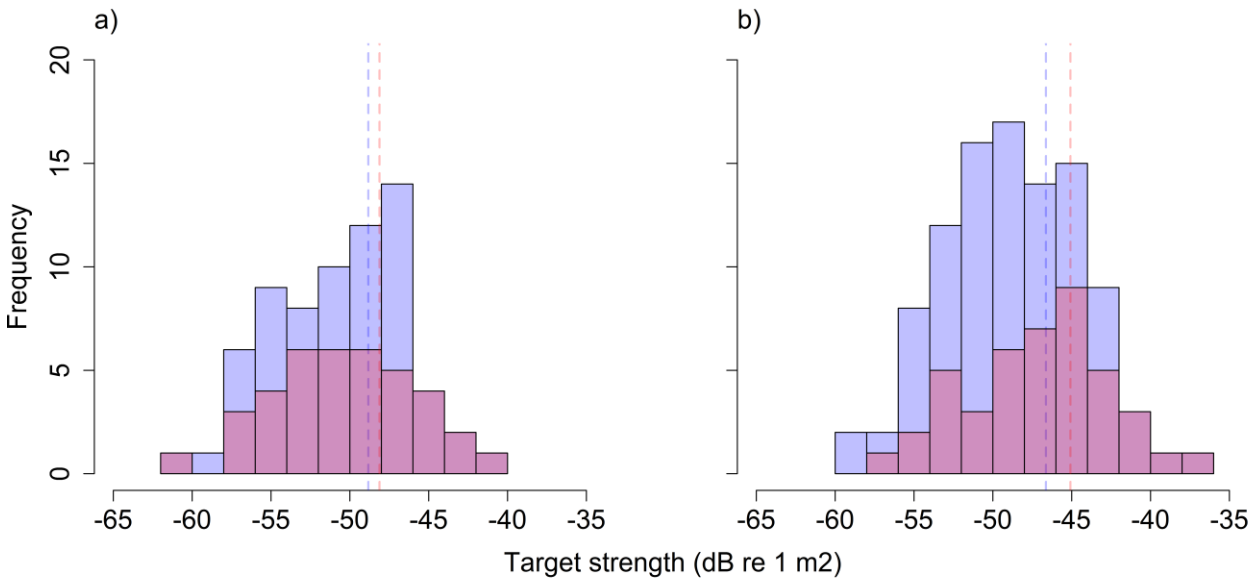

Figure 3.11 Target strength (*TS*, dB re 1 m^2) distributions at 38 kHz (a) and 120 kHz (b). The purple histograms show the distribution of all single targets and the red histograms show the distribution of targets detected at a range greater than 3 m. The dashed purple lines show the mean *TS* as calculated in the linear domain and converted back to log for all single targets (n = 68 and 100 for 38 and 120 kHz, respectively). The dashed red lines show the mean *TS* as calculated in the linear domain and converted back to log for single targets detected greater than 3 m in range (n = 38 and 43 for 38 and 120 kHz, respectively).

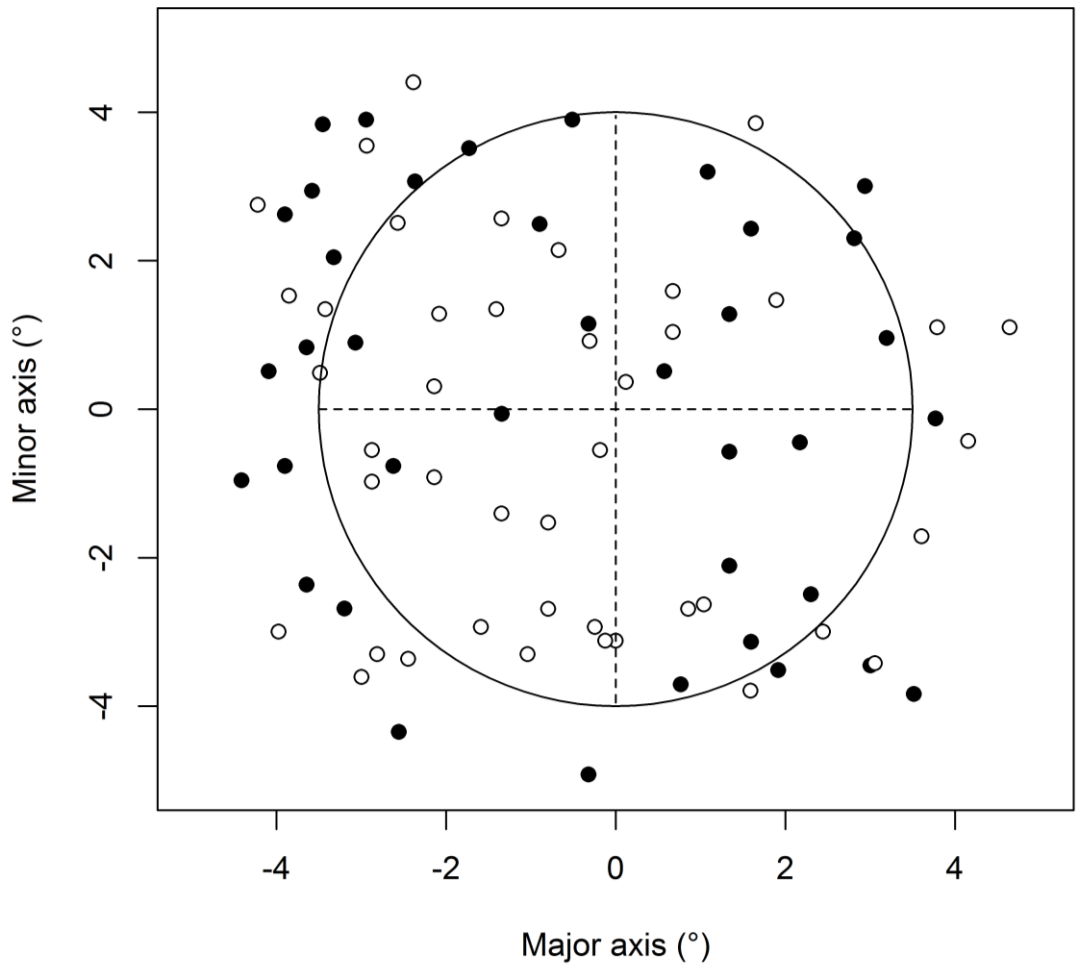

Figure 3.12 Locations of single targets in the beam at 38 kHz (filled circles) and 120 kHz (empty circles). N = 68 and 100 at 38 and 120 kHz, respectively.

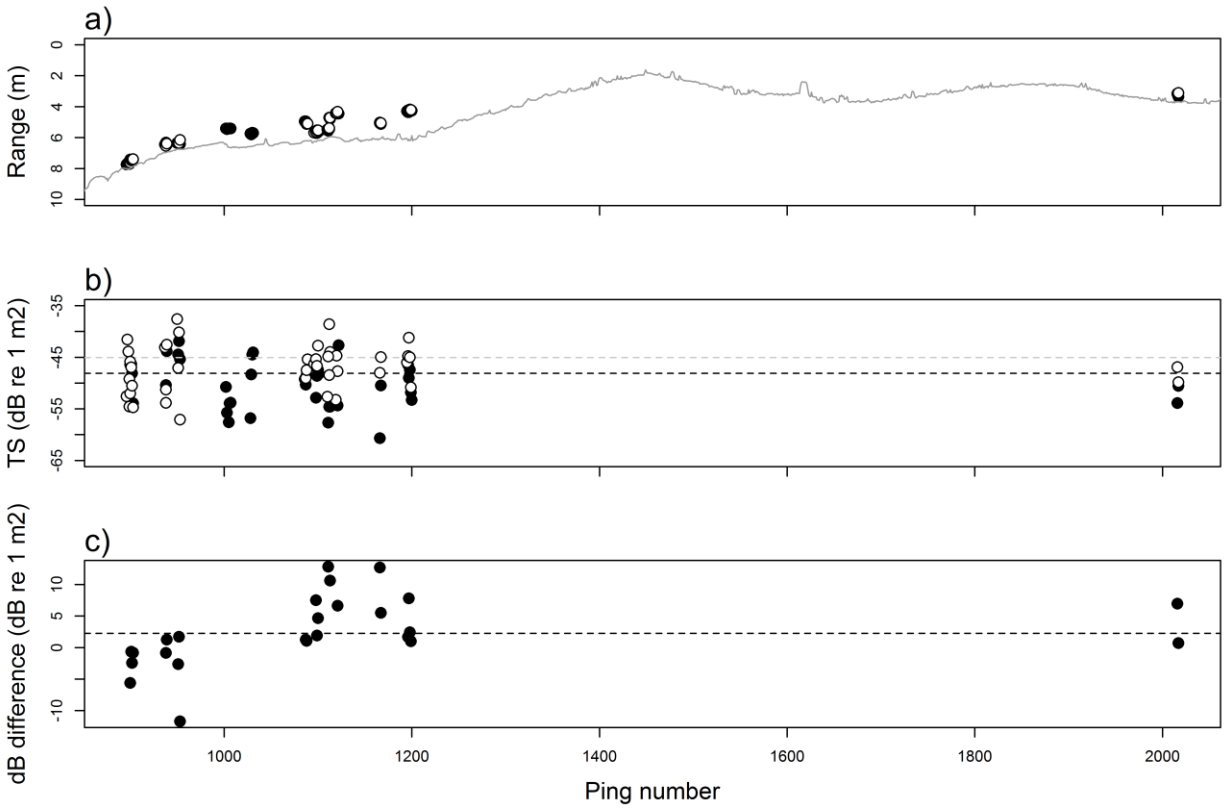

Figure 3.13 (a) Shows range of single targets from transducer versus ping number at 38 kHz (filled circle) and 120 kHz (empty circle). Grey line represents the seabed. (b) Shows the target strength (dB re 1 m^2) versus ping number at 38 kHz (filled circles) and 120 kHz (empty circles). The horizontal dashed black line is the mean *TS* at 38 kHz and the horizontal dashed grey line is the mean *TS* at 120 kHz. (c) Shows the dB difference between single targets detected at 38 and 120 kHz matched by ping number (dB difference = 120 – 38 kHz). The horizontal dashed black line shows the mean dB difference between 38 and 120 kHz. All targets shown are greater than 3 m in range from the transducer face. Only targets greater than 3 m from the transducer are shown.

Target range showed some correlation with *TS* (Figures 3.14), suggesting that there may be some near-field effects associated with this dataset. For example there is a 1.87 dB re 1 m^2 change in the mean *TS* at 38 kHz when selecting single targets from 2-3 m (n=30) and 4-5 m (n=8) and a 3.90 dB re 1 m^2 change in mean *TS* at 120 kHz for single targets from 2-3 m (n=57) and 4-5 m (n=12).

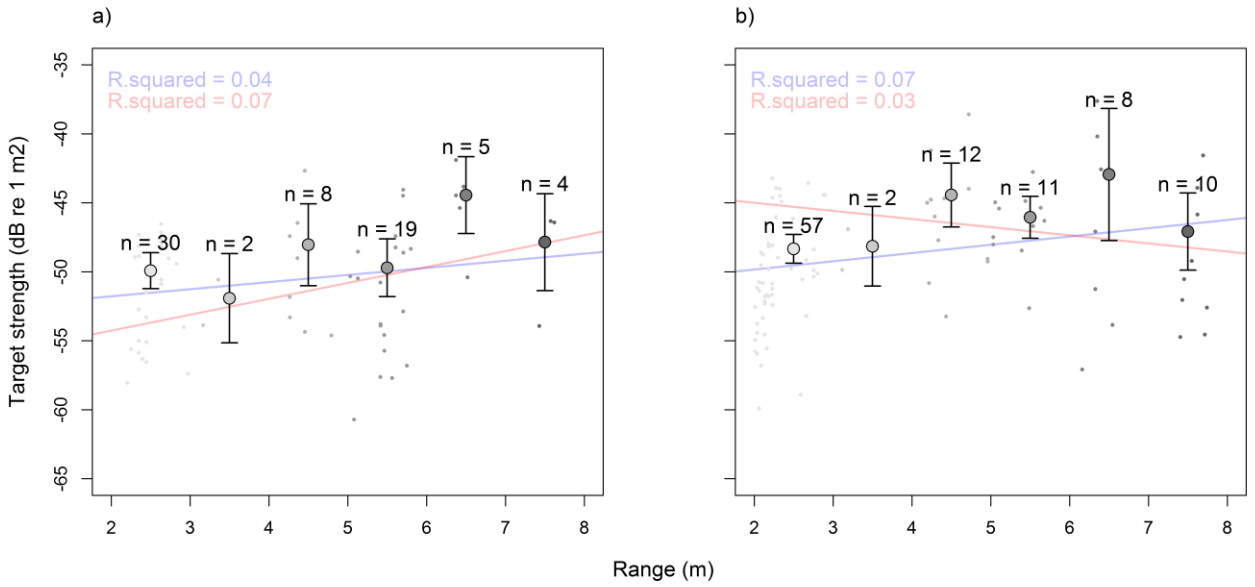

Figure 2.34 Target range against target strength (dB re 1 m^2) at (a) 38 kHz and (b) 120 kHz. The large grey circles show the mean *TS* at different range intervals and the error show the 95% confidence intervals. The colour of the individual *TS* values corresponds to the range interval they belong to. The purple lines show the linear regression between all the data points (n = 68 and 100 for 38 and 120 kHz, respectively) with the R^2 given in the top left corners (purple). The pink lines show the linear regression between targets greater than 3 m from the transducer (n = 38 and 43 for 38 and 120 kHz, respectively) with the R^2 given in the top left corners (pink).

3.2.2 Fish tracks

At 38 kHz a total of 10 fish were tracked (consisting of 50 single targets) within the confines of the tracking algorithm (Table 3.7) and 16 were tracked at 120 kHz (consisting of 81 single targets). Mean *TS* of fish tracks were -48.26 and -46.49 dB re 1 m^2 at 38 and 120 kHz, which gives a dB difference of 1.77 dB re 1 m^2, which is 1.27 dB re 1 m^2 less than suggested from single targets (3.04 dB re 1 m^2). When considering fish tracks with a mean range greater than 3 m, only 6 tracks (consisting of 25 single targets) at 38 kHz and 8 tracks (consisting of 33 single targets) at 120 kHz were detected (Table 3.7). This resulted in mean *TS* of -47.27 and -45.38 dB re 1 m^2 at 38 and 120 kHz respectively, which is a 1.89 dB re 1 m^2 difference (Table 3.7).

Five fish were tracked simultaneous at 38 and 120 kHz which resulted in mean *TS* of -47.55 and -44.20 dB re 1 m^2, respectively (dB difference 3.34 dB re 1 m^2).

Table 3.7 Mean target strength determined from target tracking at 38 and 120 kHz. N tracks is number of fish tracks and N targets is the number of single targets which make up those tracks.

	All			>3 m			Matched targets		
Frequency (kHz)	**Mean *TS* (dB re 1 m²)**	**N tracks**	**N targets**	**Mean TS (dB re 1 m²)**	**N tracks**	**N targets**	**Mean TS (dB re 1 m²)**	**N tracks**	**N targets**
38	-48.26	10	50	-47.27	6	25	-47.55	5	20
120	-46.49	16	81	-45.38	8	33	-44.20		26
dB difference (120 –38 kHz)	1.77			1.89			3.34		

3.2.3 Target strength comparison

When compared to the existing 38 kHz *TS-SL* equations for orange roughy, as given in Eqs 2.10 and 2.11, the *in situ TS* measurements shown in Tables 3.6 and 3.7 have much higher mean values. Mean *TS* determined from single targets is 2.08 and 1.99 dB re 1 m^2 higher compared to estimated *TS* for the same length orange roughy given by Eqs 2.10 and 2.11, respectively. Mean *TS* as determined from tracked orange roughy is 2.92 and 2.83 dB re 1 m^2 higher compared to estimates given by Eqs 2.10 and Eqs 2.11. These differences can result in almost a halving of fish biomass.

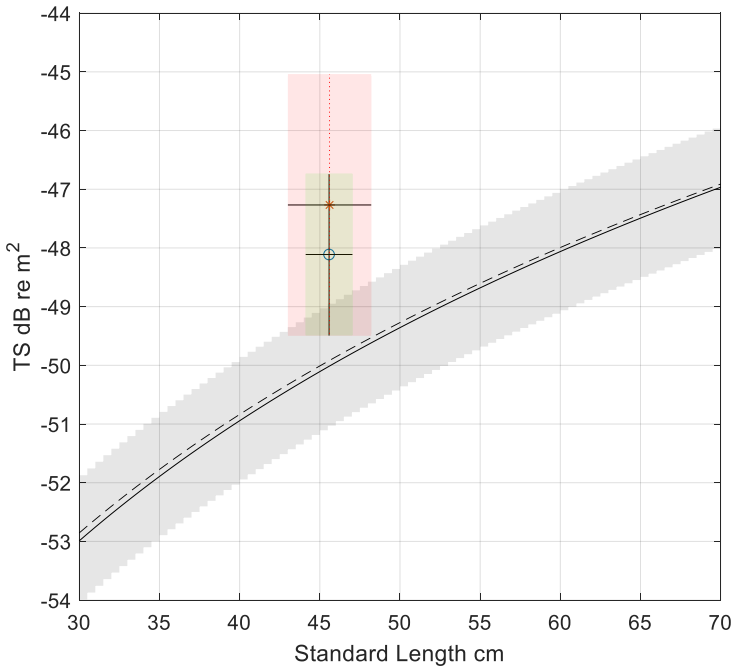

Figure 3.15 Target strength (dB re 1 m^2) versus standard length (cm). Solid line shows values derived from *TS-L* = 16.37*$\log_{10}$(*SL*)-77.17, where 16.37 is taken from McClatchie *et al.*, (1999) and 77.17 is taken from Kloser *et al.*, (2013). The dashed line shows values derived from *TS-L* = 16.15*$\log_{10}$(*SL*)-76.71 as given by Niklitschek and Patchell (2015). The solid circle represents the mean *TS* based on *in situ* single target detections of orange roughy detected at ranges greater than 3 m from the transducer with an assumed geometric mean standard length of 44.5 cm. The solid square represents the mean *TS* based on *in situ* tracked orange with mean detection ranges greater than 3 m in range with an assumed geometric mean standard length of 44.5 cm.

3.2.4 Species identification using the AOS

In 2014 the net attached Acoustic and Optical system was used successfully on the high seas by fisher's to collect species identification information. The AOS species identification using 38 kHz and 120 kHz frequencies demonstrated that the frequency difference observed on the larger 45 cm orange roughy was ≅4 dB re 1 m^{-1} (based on the black rectangles with show strong backscattering in Figure 3.16) and similar to that observed for the 35 cm fish in Australia and New Zealand. The AOS should be used in areas where species mixtures occur and or steep sloping bottoms to reduce biomass estimation bias and uncertainty.

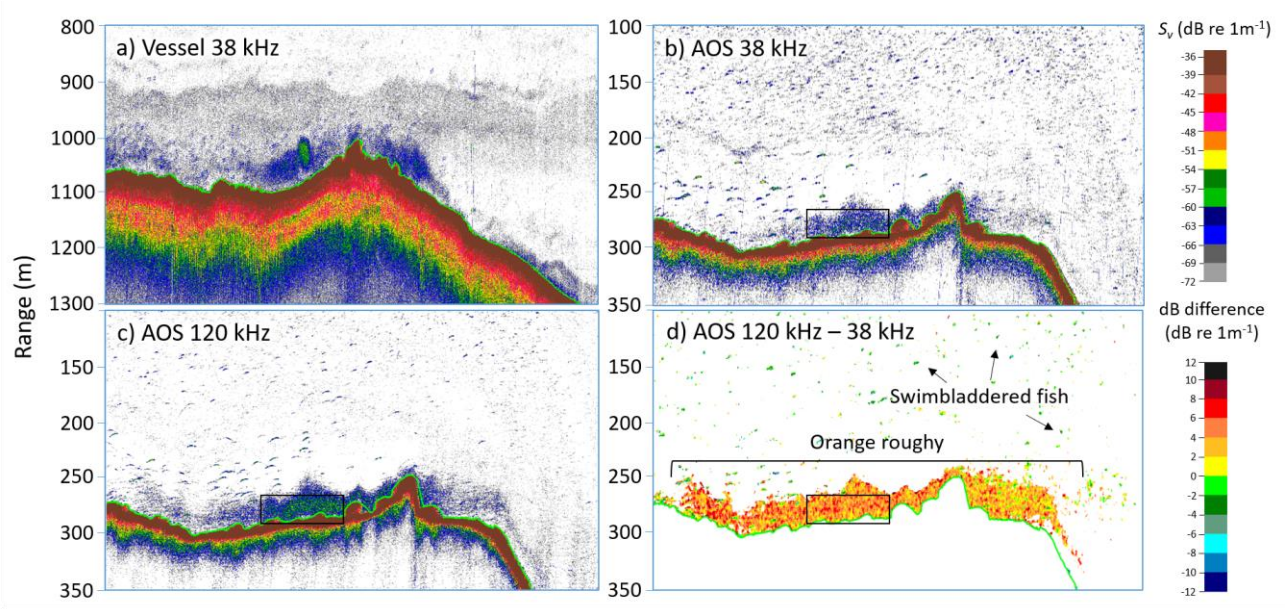

Figure 3.16 Acoustic data collected on 3rd July 2014 from *FV* Will Watch showing orange roughy aggregations, (a) vessel 38 kHz, (b) AOS 38 kHz, (c) AOS 120 kHz and (d) AOS 120 kHz minus AOS 38 kHz. Colour scales for a, b and c are S_v (dB re 1 m-1) (upper colour scale). The colour scale for d shows the dB difference between 120 and 38 kHz (lower colour scale). Orange roughy show as yellows and oranges and swimbladdered fish appear as greens and blues. The green lines shows the acoustic detected bottom. The black rectangles in b, c and d shows a region of strong backscatter where the dB difference is ≅4 dB re 1 m^{-1}.

4 Uncertainty estimates

In addition to estimates of abundance we also require some indication of the accuracy of the results. Table 4.1 provides definitions of some important terms associated with estimates of uncertainty. The information available from echo-integration surveys will include some or all of the following (Simmonds and MacLennan, 2005):

1) Acoustic data
2) Calibration
3) Size and species composition, length, sex, and weight of biological samples collected by fishing
4) Target strength and its dependence on size and orientation
5) Environmental data (e.g. water temperature and salinity at various depths)
6) The surveyed area, e.g. the cruise track, inter-transects, fishing and hydrographic stations.

Each of the above are potential sources of uncertainty in echo-integration surveys and all but number 6 are relevant to estimates of target strength. Table 4.2 provides a detailed summary of some of the uncertainties commonly encountered in echo-integration surveys and target strength studies. These include physical calibration, environmental conditions (sound speed and absorption), target strength, species identification, detection probability, as well as sampling and random error. A further discussion of the uncertainties associated with orange roughy acoustic surveys is given in Kloser *et al.*, (2018).

Table 4.1. Important definitions used in this chapter.

Term	Definition
Uncertainty	The uncertainty, when explicitly stated, describes the range of values that we expect the true value to fall within.
Error	Error is usually defined as the difference between the true and measured value. Error can include: human error (e.g. mistakes in data entry), systematic error (e.g. mistakes in survey design), and random error (e.g. caused by environmental conditions or other unpredictable factors).
Bias	Bias (also known as systematic error), which may be positive or negative, occurs when systematic error is introduced in the study. Bias can occur at any phase, including survey design or data collection, as well as in the process of data analysis and publication. Bias is sometimes defined as the amount of accuracy.
Random error	Random errors occur due to chance and may be caused by, for example, small changes in an instruments performance, the environment, or the way a measurement is read, that do not cause the same error every time.
Systematic error	Systematic error (or bias) is any systematic process in the conduct of a study that results in the difference between the values that were obtained and the true value and refers to deviations that are not due to chance alone. Systematic errors result from, calibration errors or survey design, for example. Because it is a systematic process, it will cause a distortion from the truth in a predictable (i.e. not random) way.
Accuracy	Accuracy describes the degree of closeness of measurements of a quantity to that quantity's true value.
Precision	The precision of a measurement system, related to reproducibility and repeatability, is the degree to which repeated measurements under unchanged conditions show the same results.
Variability	The amount of imprecision.

1 **Table 4.2. Summary of uncertainty associated with echo-integration surveys and target strength measurements from vessel surveys.**

Source of error	Random	Systematic	Factor	What is the problem?	How do we mitigate?	Considerations
Physical calibration	X	X	0.9 to 1.1 (on axis calibration) 0.8 to 1.2 (calibration of beam)	- If the calibration is wrong, the abundance estimate will be consistently different from the true value; a bias is introduced, which may be positive or negative. -Bias can be introduced in a number of ways, including: system gain, equivalent beam angle, density and composition of sphere, position of sphere in beam, system electronics, ageing effects, non-linear effects, signal-to-noise and biological contamination (i.e. biology in the water interferes with the signal from the sphere).	- Calibrate annually (ideally every time a survey is carried out). - Calibrate close to where the survey is being carried out. - Calibrate when fewest biological targets are present (e.g. during the day when diurnal migration is at its lowest). - Calibrate in favourable conditions (e.g. minimal tide, wind and wave action). - Develop standard report format. - Measure the equivalent beam angle of the transducer. - Monitor transceiver/transducer stability by carrying out repeat transects over the same area of sea floor.	- Lower frequencies can be measured more reliably. - Use the appropriately sized sphere.
Transducer (vessel) motion	X	X	1.0 to 1.2	- Vessel motion (due to bad weather) leads to differences in the pointing direction of the transducer between transmission and reception. The acoustic biomass will be biased low if this not accounted for.	- Collect motion reference data and apply the Dunford (2005) motion correction algorithm to the data. - Restrict data collection to periods of calm. - Use a stable deep-towed system.	- Narrow beams are more sensitive to motion.
Bubble attenuation	X	X	1.0 to 1.1	- Acoustic signals become attenuated by air bubbles beneath the transducer (often caused by bad weather) and can compromise data quality meaning that echo integration results may underestimate abundance. Note that attenuation is always negatively biased.	-Keel mounted and deep-towed systems are less sensitive. - Restrict surveying to good weather. - Apply filters which locate and remove attenuated pings (Ryan *et al.*, 2015).	- It is not considered appropriate to merely apply a correction factor to the data without understanding how significant the attenuation is. Nor is it appropriate to interpolate attenuated pings by replacing the value with the values of the surrounding pings. Attenuated pings should instead be removed from analysis.
Environmental condition			-	- Sound propagation is affected by the values of sound speed (c_w) and absorption coefficient (α_α). These values are not constant throughout the water column (changing with depth/range, temperature and salinity), however, at present, only a single value can be applied during acoustic data processing in Echoview.	- Carry out CTD deployments at time and location of the survey. - Use deep towed systems.	- Long range and high frequencies suffer more from uncertainty in absorption coefficients. - Less of an issue for shallow water surveys, where high levels of mixing can occur.

Absorption (attenuation coefficient) and sound speed		X		- It is not appropriate to use surface estimates of c_w and α_α, when fish are >1000 m in depth, nor is it correct to use a value recorded at >1000m.	- Use cumulative mean values for sound speed and absorption coefficient when analysing acoustic data. - Determine absorption correction factors over the depth range being investigated.	
			1 to 1.31	- Differences in absorption using Francois and Garrison (1982) and Doonan *et al.* (2003).	- *In situ* measurements of absorption coefficient are required to identify whether Francois and Garrison (1982) or Doonan *et al.* (2003) is more appropriate for deep-sea vessel-based acoustic surveys.	- In order to be conservation, Doonan *et al.* (2003) may be considered acceptable.
Target strength	X	X	0.63 to 1	- Existing *TS-L* equations based on smaller orange roughy (mean length 35 cm). - Issues have been identified with measuring orange roughy *TS* using the AOS system, including, near-field of transducer and fish, long pulse duration (and thus low sampling resolution), and narrow beamwidth meaning the fish are not being fully ensonified at close range (i.e. <4m).	- Target strength measurements required for larger orange roughy *in situ* (expand on the work done in this report). - Use wider beamwidth to reduce near-field of transducer and reduce detection range. - Use short pulse duration to improve sampling resolution.	- Target strength is considered a stochastic variable (a variable whose value is subject to variations, the source of which may be unknown) and can have a wide range of values described by a probability function. - Target strength is governed by qualities such as: geometry, physiology, angle of orientation and properties of materials, all of which are largely unknown. - It is uncertain whether target strength values measured are representative of the population being surveyed, or whether it represents a subset of the population.
Species identification	X		0.8 to 1.1	- School delineation. Accurately defining the edges of an aggregation. - Mixed species assemblages. For example, inclusion of non-orange roughy targets during echo integration (e.g. inclusion of swim-bladdered fish during echo integration will lead to an underestimate of abundance). - Lack of biological data to assist in disaggregation of acoustic values.	- Potential based on previous work due to gas bladders-errors in New Zealand/Australia. - Use of multiple frequencies or broadband echosounders. - Directed biological samples. - Use of dB differencing algorithm	- Depends on species mix and target strength differences among species.
Detectability	X	X	-	- The availability of fish to the acoustics with additional survey sampling variability is inevitably a factor.	- Reduce range between transducer and fish. - Use noise limited platforms. - Conduct surveys when fish are aggregated for spawning and preferably when they become fully available to the acoustics.	- Less of a problem for low frequencies.

Detection probability	X	X		- Thresholding: too low a display threshold may include loosely scattered non-orange roughy targets, whereas, too high a display threshold is likely to exclude orange roughy from analysis, leaving only strong (likely swimbladdered) targets.	- A S_v display threshold between -75 and -39 dB re 1 m^{-1} may be considered suitable for orange roughy (as used in this report)..	- Note that this threshold is purely visual and does not affect the underlying acoustic values.
			-	- Poor signal-to-noise can affect detectability at range. Dispersed fish may not be distinguishable from noise.		
Survey design/inference area	X		0.7 to 1.3	- Incomplete survey coverage of the region within years and between surveys. - Large variation within years not related to observation error. - Difference between methods described by Jolly and Hampton, the conventional EDSU method and geostatistical methods. - Survey area assumptions and proportion of the area differences between methods and extrapolation.	- Use geostatistics to estimate survey error - Highly variable series – need methods to accept surveys with similar complete coverage - Define a target survey area (where the stock is expected to be) for each ground. -Target a minimum of three grounds within a year to reduce the overall CV.	- Depends on spatial distributions; layers can be estimated precisely; highly variable school sizes are the most difficult scenario
Dead-zone calculation	X		0.8 to 1.2	- The acoustic deadzone (or shadow zone) is a region adjacent to the seabed where it is not possible to distinguish signal from the water column (e.g. orange roughy aggregations) with signal from the seabed (Kloser, 1996) and is caused by physical characteristics of the transmit pulse, the acoustic beam (Ona and Mitson, 1996) and by the gradient of the seabed (Kloser, 1996).	- Use method described by Kloser (1996) as implemented in Echoview. - Use deep-towed system, e.g. AOS.	- Fish move into and out of the DZ - Low biomass for some surveys - Variable between surveys – process error
Fish migration/movement		X	0.8 to 1.2	- Fish move within the survey area which can lead to double counting or undercounting. - Variable between surveys and between years. -This could be significant to estimates of biomass.	-Investigate movement at the time of the survey. -Survey when aggregations are stationary. -Survey design that mitigate effects of fish movement (e.g. interlaced transects) and or analytical strategy to decrease effect (e.g. splitting surveys).	- Surveys should be considered for assessment with respect to movement levels. Too much movement may mean surveys are dropped.
Diurnal behaviour	X		-	- At night fish may move up in the water column, dispersing as they do so. This makes them more difficult to detect.	- Run acoustic surveys when fish are most aggregated.	- Greatest for major vertical migration with changes in target strength due to ambient pressure variation
Avoidance reactions		X	-	- Fish may react negatively to the presence of a vessel or towed-body system. In turn this can negatively affect abundance estimates as fish may move outside of detection area or	- Avoid getting too close to schooling aggregations of fish.	- Not relevant to vessel based acoustic surveys of deep sea fish. Becomes more of a problem when the platform is lowered close to aggregations.

				swim in a downward (or upward) direction which reduces their surface area and thus *TS* which reduces detectability.	- Limit size of towed systems to limit any pressure waves generated. - Use silent vessels and towed systems.	- Low with quiet vessels in open water, worse in confined and swallow schooling species.
Biological			-	- Lack of directed biological sampling.	- Take multiple direct biological samples of the survey population.	
Length estimates	X	X	-	- Are net samples representative of the surveyed population? - Important for applying the correct *TS* to biomass estimates.	-Take regular biological samples	
Length-weight relationship		X	-	- Existing length-weight relationships (i.e. Lyle *et al* (1991) and Kloser *et al* (2017)) are derived from a smaller size range of orange roughy and may not be appropriate for larger fish.	- Determine new length-weight relationship for size range being studied, as done in this report (although it is not clear if the scales used are biased). - Ideally establish a new length-weight relationship for each survey.	- Effect may be different for male and females.

2

5 References

Blackman, S. S. 1986. Multiple-target tracking with radar applications, Artech House.

Demer, D. A. 2004. An estimate of error for the CCAMLR 2000 survey estimate of krill biomass. *Deep-Sea Research Part II-Topical Studies in Oceanography*, 51: 1237–1251.

Demer, D.A., Berger, L., Bernasconi, M., Bethke, E., Boswell, K., Chu, D., Domokos, R., *et al*. 2015. Calibration of acoustic instruments. ICES Cooperative Research Report No. 326. 133 pp.

Demer, D. A., Soule, M. A., and Hewitt, R. P. 1999. A multiple-frequency method for potentially improving the accuracy and precision of in situ target strength measurements. *Journal of the Acoustical Society of America*, 105(4): 2359-2376.

De Robertis, A., and Higginbottom, I. 2007. A post-processing technique to estimate the signal-to-noise ratio and remove echosounder background noise. *ICES Journal of Marine Science*, 64: 1282–1291.

Doonan, I. J., Coombs, R. F., and McClatchie, S. 2003. The absorption of sound in seawater in relation to the estimation of deep-water fish biomass. *ICES Journal of Marine Science*, 60: 1047–1055.

Dunford, A. J. 2005. Correcting echo-integration data for transducer motion (L). *Journal of the Acoustical Society of America*, 118: 2121-2123.

Echoview Software Pty Ltd, 2015. Echoview Software 8.0.84. Echoview Software Pty Ltd, Hobart, Australia.

FAO 2017. Workshop to review orange roughy acoustic data. ABNJ Deep Sea Project, 30th Jan - 3rd Feb 2017 Rome Italy 13pp.

Francois, R. E., and Garrison, G. R. 1982b. Sound absorption based on ocean measurements. Part II: Boric acid contribution and equation for total absorption. *Journal of the Acoustical Society of America*, 72: 1879–1890.

Gastauer, S., Scoulding, B., and Parsons, M. 2017. Towards acoustic monitoring of a mixed demersal fishery based on commercial data: The case of the Northern Demersal Scalefish Fishery (Western Australia). *Fisheries Research*, 195: 91-104.

Guiblin, P., Rivoirard, J., and Simmonds, E. J. 1995. Analyse structural de donnees a distribution dissymetrique exemple du hareng ecossais. *Cahiers De Geostatistique*, 5: 137–160.

IMOS 2017. https://portal.aodn.org.au/.

Keith, G.J., Ryan, T.E., Kloser, R.J., 2005. ES60adjust.jar. Java Software Utility to Remove a Systematic Error in Simrad ES60 Data. CSIRO Marine and Atmospheric Research Hobart, Castray Esplanade, Tasmania, Australia. https://bitbucket.org/gjm/calibration-code/wiki/Home.

Kloser, R. J. 1996. Improved precision of acoustic surveys of benthopelagic fish by means of a deep-towed transducer. *ICES Journal of Marine Science*, 53: 407–413.

Kloser, R. J., Macaulay, G. J., Ryan, T., and Lewis, M. 2013. Identification and target strength of orange roughy (*Hoplostethus atlanticus*) measured *in situ*. *Journal of the Acoustical Society of America*, 134: 97-108.

Kloser, R.J., Scoulding, B., Niklitschek, E., Toledo, P., and Patchell, G. 2018. Orange roughy biomass estimation in SIOFA: Review of the use of acoustics from industry vessels.

Kloser, R.J., Sutton, C. Kunnath, H. and Downie, R. 2017 Orange roughy eastern zone spawning biomass 2016. Report to South East Trawl Industry Association. Copy held at CSIRO Marine and Atmospheric Research, Hobart.

Macaulay, G.J., Kloser, R. J., and Ryan, T.E. 2013. *In situ* target strength estimates of visually verified orange roughy. *ICES Journal of Marine Science*, 70: 215-222.

Mackenzie, K.V. 1981. Nine-term equation for sound speed in the oceans. *Journal of the Acoustical Society of America*, 70: 807-812.

MacLennan, D. N. 1990. Acoustical measurement of fish abundance. *Journal of the Acoustical Society of America*, 87: 1-15.

MacLennan, D.N., Fernandes, P.G., and Dalen, J. 2002. A consistent approach to definitions and symbols in fisheries acoustics. *ICES Journal of Marine Science*, 59: 365-369.

Matheron, G. 1971. The theory of regionalised variables and its applications. Cahiers du centre de Morphologie Mathematique, Fontainebleau 5 (Ecole Nationale Superiore des Mines de Paris, Paris, France).

McClatchie, S., Macaulay, G. J., Coombs, R., Grimes, P., and Hart, A. 1999. Target strength of an oily deep-water fish, orange roughy In situ target strength estimates of visually verified orange roughy (Hoplostethus atlanticus). Part I. Experiments. *Journal of the Acoustical Society of America*, 106: 131–142.

McClatchie, S., and Ye, Z. 2000. Target strength of an oily deep-water fish, orange roughy (*Hoplostethus atlanticus*) II. Modelling. *Journal of the Acoustical Society of America*, 107(3): 1280-1285.

Niklitschek, E.J. and Patchell, G. 2015. *Acoustic abundance indexes for orange roughy and alfonsino in the Indian Ocean (SIOFA) from industry acoustics 2004 – 2008*. Southern Indian Ocean fisheries Agreement Scientific Committee Report. SIOFA SC-01-INFO-15.

Ona, E., and Mitson, R. B. 1996. Acoustic sampling and signal processing near the seabed: the deadzone revisited. *ICES Journal of Marine Science*, 53(4): 677-690.

R Core Team, 2017. R: A Language and Environment for Statistical Computing. R Foundation for Statistical Computing, Vienna, Austria. URL https://www.R-project.org/.

Renard, D., Bez, N., Desassis, N., Beucher, H., Ors, F., and Laporte, F. 2015. RGeostats: The Geostatistical package 11.0.1. MINES ParisTech.

Rivoirard, J., Simmonds, J., Foote, K. G., Fernandes, P. and Bez, N., 2000. Geostatistics for estimating fish abundance. Blackwell Science, Oxford, pp 25 - 40.

Ryan, T. E., and Cordell, J. 2014. Development and application of acoustic-optical technology for sustainable deep-sea fishing – AOS calibration and metadata report – Mauritius September 2014.

Ryan, T.E., Downie, R.A., Kloser, R.J., Keith, G., 2015. Reducing bias due to noise and attenuation in open-ocean echo integration data. *ICES Journal of Marine Science*, 72, 2482–2493.

Ryan, T. E., and Kloser, R. J. Improved estimates of orange roughy biomass using an acoustic-optical system in commercial trawlnets. *ICES Journal of Marine Science*, 73: 2114-2126.

Ryan, T. E., Kloser, R. J., and Macaulay, G. J. 2009. Measurement and visual verification of fish target strength using an acoustic-optical system attached to a trawlnet. *ICES Journal of Marine Science*, 66: 1238–1244.

Scoulding, B., Gastauer, S., MacLennan, D. N., Fassler, S. M. M., Copland, P. and Fernandes, P. G. Effects of variable mean target strength on estimates of abundance: the case of Atlantic mackerel *(Scomber scombrus*). *ICES Journal of Marine Science*, 74: 822-831.

Simmonds, J. E. and MacLennan, D. N. 2005 Fisheries Acoustics: Theory and Practice, 2nd ed. Oxford: Blackwell Science Ltd.

Soule, M. A. 2005. Calibration of the Simrad ES60 echosounder on the F/V Will Watch. Mauritius – 05 November 2005. Fisheries Resource Survey cc.

Soule, M. A. 2009. Calibration of the Simrad ES60 echosounder on the F/V Will Watch. Mauritius – 31 May 2009. Fisheries Resource Survey cc.

Woillez, M., Rivoirard, J., and Fernandes, P.G. 2009. Evaluating the uncertainty of abundance estimates from acoustic surveys using geostatistical simulations. *ICES Journal of Marine Science*, 66: 1377-1383.

Woillez, M., Walline, P.D., Ianelli, J.N., Dorn, M.W., Wilson, C.D., Punt, A.E., 2016. Evaluating total uncertainty for biomass-and abundance-at-age estimates from eastern Bering Sea walleye pollock acoustic-trawl surveys. *ICES Journal of Marine Science*, 73, 2208–2226.

CONTACT US

t 1300 363 400
+61 3 9545 2176
e csiroenquiries@csiro.au
w www.csiro.au

AT CSIRO, WE DO THE EXTRAORDINARY EVERY DAY

We innovate for tomorrow and help improve today – for our customers, all Australians and the world.

Our innovations contribute billions of dollars to the Australian economy every year. As the largest patent holder in the nation, our vast wealth of intellectual property has led to more than 150 spin-off companies.

With more than 5,000 experts and a burning desire to get things done, we are Australia's catalyst for innovation.

CSIRO. WE IMAGINE. WE COLLABORATE. WE INNOVATE.

FOR FURTHER INFORMATION

Oceans and Atmosphere
Ben Scoulding
t +61 3 62325366
e ben.scoulding@csiro.au
w www.csiro.au

Oceans and Atmosphere
Rudy Kloser
t +61 3 62325000
e rudy.kloser@csiro.au
w www.csiro.au